Cell separation and culture conditions

Human basophils were isolated from venous blood obtained from consenting volunteers with no history of atopic diseases. Basophils were semipurified by Percoll density gradient centrifugation as previously described (18). The purity of semipurified basophil preparations was 12.5 ± 0.13% (n = 60). A vast majority of the contaminating cells were lymphocytes and monocytes, and the preparations usually contained no eosinophils. Their viability, measured by the trypan blue exclusion test, was consistently >95%. In some experiments basophils were further purified (purity, ~98%) by negative selection with MACS beads (Basophil Isolation kit; Miltenyi Biotec, Auburn, CA) as described previously (13).

HUVEC were isolated and cultured according to the previously described methods (19). The culture medium was medium 199 (Invitrogen Life Technologies, Grand Island, NY) supplemented with 20% FCS (Invitrogen Life Technologies), 2 mM L-glutamine (Invitrogen Life Technologies), antibiotics (100 U/ml penicillin and 100 μg/ml streptomycin; Invitrogen Life Technologies), endothelial cell growth supplement (20 μg/ml; Collaborative Research, Bedford, MA), and heparin sodium (90 μg/ml; Sigma-Aldrich). HUVEC (2–5 × 10^4 cells) were cultured on 2% gelatin-coated Transwell culture inserts (6.5-mm diameter polycarbonate membranes with 5-μm pores; Costar, Cambridge, MA) for 2–5 days. To confirm the confluence of the HUVEC on the membrane, sample monolayers were routinely stained with Diff-Quick (International Reagents, Kobe, Japan) before use in each experiment.

TEM assay

Unless otherwise indicated, HUVEC monolayers grown in Transwell inserts were pretreated for 4 h with human rIL-1β (5 ng/ml; Diaclone Research, Besaçn, France) and washed twice with PIPES ACM buffer (25 mM PIPES, 119 mM NaCl, 5 mM KCl, 2 mM Ca^{2+}, 0.5 mM Mg^{2+}, and 0.03% human serum albumin). Percoll-separated basophils (3 × 10^4/100 μl) suspended in PIPES ACM buffer were added to the upper wells, and samples to be tested (600 μl) were placed in the lower wells. After incubation for 3 h at 37°C, the cells that had migrated to the lower wells were collected and washed twice in PBS supplemented with 3% FCS and 0.1% NaN_3. For analysis of the numbers of migrated basophils, the cells were stained with FITC-conjugated goat anti-human IgE (BioSource International, Camarillo, CA) at 4°C for 30 min. After washing the cells, the numbers of FITC-positive cells were counted by flow cytometry as previously described (13). Basophil TEM was expressed as a percentage of the number of inoculated basophils.

The effects of integrins and CCRs were examined by treating cells with blocking mAbs or controls at 37°C for 30 min. Without washing, treated cells were placed in the upper wells. We used $F(ab')_2$ for blocking CD54 (ICAM-1) and CD106 (VCAM-1) on HUVEC to avoid the undesired effects of the Fc portion of immobilized mouse mAb on basophil FcγR. HUVEC were pretreated with the $F(ab')_2$ of each mAb or controls at 37°C for 30 min before assay. The inhibition by mAbs was calculated using the following formula: % inhibition = (migration by isotype-matched control-treated cells − migration by blocking mAb-treated cells)/(migration by isotype-matched control-treated cells) × 100.

Statistics

All data are expressed as the mean ± SEM, and differences between values were analyzed by the one-way ANOVA. When this test indicated a significant difference, Fisher's protected least significant difference test was used to compare individual groups.

Results

Effects of IL-1 and eotaxin on basophil migration across endothelial cells

A basophil TEM assay was performed using Percoll-separated basophils and Transwell systems with cultivated HUVEC on the surface. In accordance with the previous reports of eosinophil TEM assays (19), HUVEC were activated by stimulation with IL-1β for 4 h before assays. As shown in Fig. 1*A*, only marginal numbers of basophils had transmigrated across a layer of unstimulated HUVEC even after 3 h of incubation. In contrast, stimulation of HUVEC with IL-1β significantly enhanced basophil TEM at later time points. During the initial 2 h, TEM across IL-1-activated HUVEC showed a similar time course of accumulation as TEM across unstimulated HUVEC. After 3-h incubation, however, the

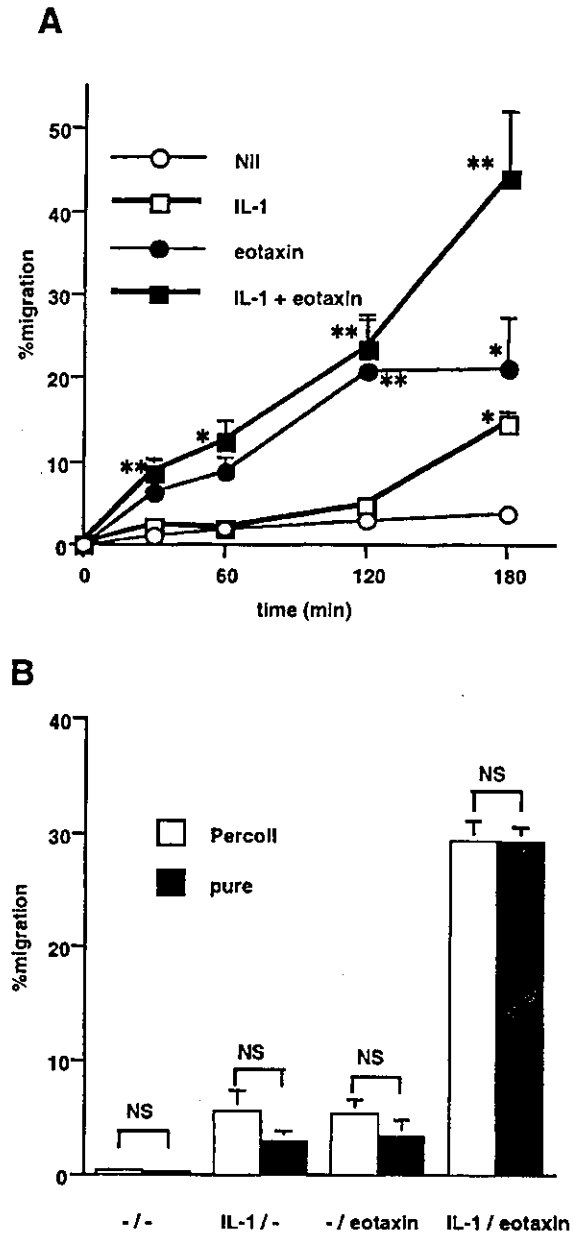

FIGURE 1. Time course of TEM of basophils. *A*, HUVEC monolayers in Transwell inserts were pretreated with (■ and □) and without (● and ○) IL-1-β (5 ng/ml) at 37°C for 4 h. Percoll-separated basophils were added to the upper wells, and the chambers were incubated at 37°C in the presence (■ and ●) and the absence (□ and ○) of eotaxin (5 nM) in the lower wells. After the indicated time periods, the cells in lower wells were collected, and the number of IgE-positive cells was determined by flow cytometry. Bars represent the SEM (n = 6–8). *, $p < 0.05$; **, $p < 0.01$ (vs spontaneous migration (○) at corresponding time point). *B*, TEM through HUVEC by highly purified basophils was indicated. Basophils from a sample of Percoll-separated cells were further enriched by negative selection with MACS beads. TEM assays were performed for 3 h, as described above, using Percoll- (□) and MACS-separated (■) basophils. The purities of Percoll- and MACS-separated basophils were 19.6 ± 5.7 and 98.3 ± 0.4%, respectively. Bars represent the SEM (n = 5). NS, no significant difference between Percoll- and MACS-separated basophils.

number of transmigrated cells was significantly increased in cultures stimulated with IL-1β (3.9 ± 1.2 and 14.7 ± 2.7%, for TEM across unstimulated and IL-1-stimulated HUVEC, respectively). Furthermore, basophil TEM was markedly enhanced by the presence of

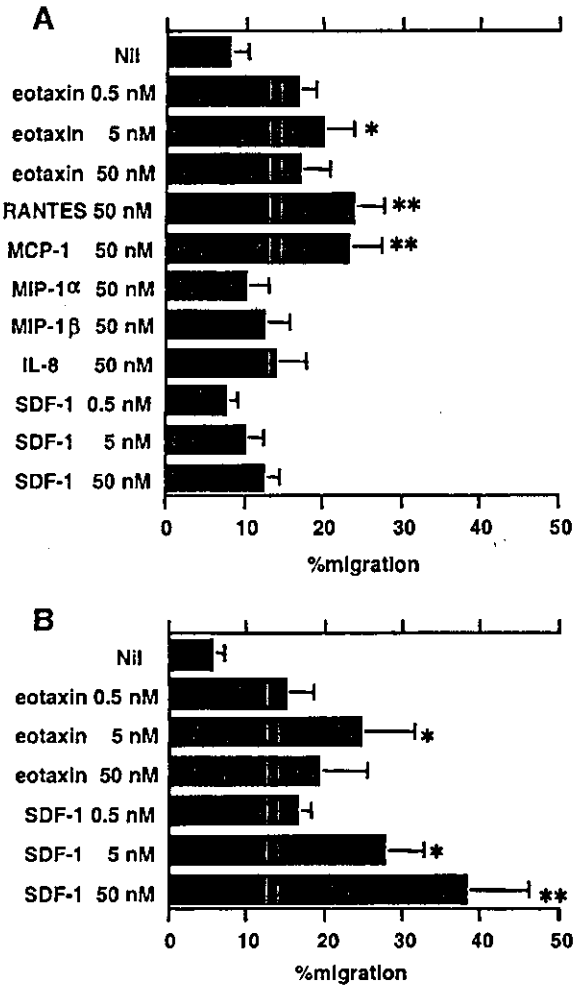

FIGURE 2. Effects of chemokines on basophil TEM. *A*, HUVEC were pretreated with IL-1-β (5 ng/ml) at 37°C for 4 h. A basophil TEM assay was performed in the presence of various chemokines in the lower wells. Basophils were separated by Percoll and immediately added to the upper wells. After 3 h of incubation at 37°C, the cells in the lower wells were collected, and the number of IgE-positive cells was determined by flow cytometry. *B*, Percoll-separated basophils were cultured in RPMI 1640 supplemented with 10% FCS and antibiotics at 37°C for 24 h. The cultured cells were added to the upper wells, and TEM assay was performed as described above. Bars represent the SEM ($n = 4$–7). *, $p < 0.05$; **, $p < 0.01$ (vs migration in the absence of chemokines (Nil)).

a chemoattractant, eotaxin/CCL11. Compared with spontaneous TEM, chemokine-induced TEM showed a faster time course of accumulation. Even with unstimulated HUVEC, the number of transmigrated cells increased linearly until 2 h and then plateaued. Although a similar time course of accumulation was observed with activated HUVEC until 2 h of incubation, the number of transmigrated cells was significantly increased at 3 h of incubation (Fig. 1*A*). The basophil preparations used in these experiments were Percoll-separated and consisted of ~90% contaminating cells. To explore whether these contaminating cells indirectly affect basophil TEM, we further purified the Percoll-separated cells by negative selection with MACS beads (purity, >98%) and compared the TEM between Percoll- and MACS-separated basophils. As shown in Fig. 1*B*, no significant difference in TEM was observed between the two preparations, indicating that contaminating cell populations do not significantly affect the basophil TEM.

Basophil TEM by chemokines

The results of our and other laboratories have demonstrated the expression of multiple chemokine receptors in basophils (13, 16, 20), and our previous functional survey demonstrated that CCR3 ligands are mainly responsible for the migratory responses of resting basophils (13). Fig. 2 depicts the effects of various chemokines on basophil TEM. Transmigration was determined after 3 h of incubation using IL-1-activated HUVEC. CCR3 ligands, eotaxin, and RANTES/CCL5 induced strong basophil TEM. Eotaxin binds specifically and exclusively to CCR3, whereas RANTES binds to CCR1 with higher affinity than to CCR3. To determine the chemokine receptors responsible for RANTES-induced basophil TEM, we performed blocking experiments using receptor-specific mAbs of an antagonistic nature. As shown in Fig. 3, eotaxin-induced TEM was almost completely inhibited by anti-CCR3 mAb. Although RANTES-induced TEM was also markedly blocked by anti-CCR3 mAb, treatment with anti-CCR1 mAb exerted virtually no effect on the migratory response.

Our previous study using a HUVEC-free Transwell system demonstrated that CXCR1/CXCR2 ligand IL-8/CXCL8 and CCR2 ligand MCP-1/CCL2 also induced significant, but weak, migration of basophils (13). However, no statistically significant TEM was observed in cells stimulated with IL-8. In contrast, MCP-1 was capable of inducing TEM as strongly as eotaxin. Furthermore, a CXCR4-specific ligand, stromal cell-derived factor-1 (SDF-1)/CXCL12, was also capable of inducing strong basophil TEM under certain conditions. In our previous report we demonstrated that the expression of functional CXCR4 is induced on the basophil surface by 24 h of culture, and SDF-1 induced significant migratory responses in 24-h cultured basophils (13). The same situation was observed in TEM; although freshly isolated basophils failed to exhibit TEM in response to SDF-1, strong TEM, comparable to that induced by eotaxin, was observed with 24-h cultured basophils (Fig. 2*B*).

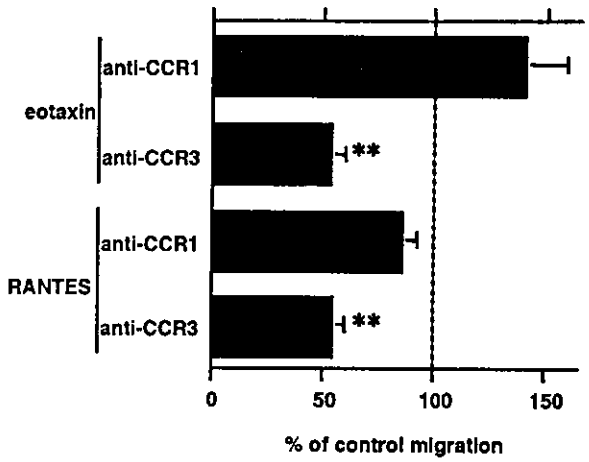

FIGURE 3. Effects of chemokine receptor blocking on chemokine-induced basophil TEM. HUVEC were pretreated with IL-1-β (5 ng/ml) at 37°C for 4 h. Percoll-separated basophils were preincubated with anti-chemokine receptor mAbs (20 μg/ml) or isotype control mAb (mouse IgG1, 20 μg/ml) at 37°C for 30 min. TEM assay was performed in the presence and the absence of eotaxin (15 nM) or RANTES (15 nM) in the lower wells for 3 h. Migrations of control Ab-treated basophils toward eotaxin and RANTES were 29.5 ± 4.6 and 28.5 ± 5.7%, respectively. Spontaneous migration without any chemokine was 9.2 ± 2.5%. Bars represent the SEM ($n = 9$). **, $p < 0.01$ (vs percentage of control migration).

Basophil TEM by IL-3

Results from our and other laboratories have established that IL-3 stimulates various aspects of basophil functions, such as mediator release (21, 22) and in vitro survival (23, 24). Furthermore, our earlier study using Boyden chamber systems demonstrated that IL-3 potently enhances in vitro locomotive responses by basophils (11). The migratory response induced by IL-3 was chemokinetic rather than chemotactic. When serially diluted IL-3 was added to the upper wells of a Transwell, we observed that the number of transmigrated basophils increased in a dose-dependent fashion (Fig. 4). A significant increase in basophil TEM was observed when the cell suspension in the upper wells contained as little as 3 pM IL-3. When the IL-3 gradient was diminished by adding the same concentration of IL-3 to both the upper and lower wells, the basophil TEM was not significantly affected. In contrast, elimination of the eotaxin gradient mostly inhibited the increase in basophil TEM, indicating that eotaxin-induced TEM was mainly chemotactic (Fig. 4). Furthermore, IL-3 showed an additive effect on eotaxin-induced TEM; the number of transmigrated cells induced by eotaxin was significantly increased in the presence of IL-3 (17.7 ± 4.4 and 23.4 ± 4.6%, eotaxin-induced TEM for the absence and the presence of IL-3, respectively; $n = 4$; $p < 0.05$).

Effects of adhesion molecules on basophil TEM

Adhesion molecules and their counter-receptors play a critical role in the TEM of various cell types. Previous studies by others revealed that basophils express both β_1 (CD49d, CD49e, and CD29) and β_2 (CD11a, CD11b, and CD18) integrins on their surface (25). When the effects of β_1 and β_2 integrins on basophil TEM across IL-1-stimulated HUVEC were studied using blocking mAbs, significant inhibition of spontaneous TEM was observed in cells treated with anti-CD18 mAb, but not in those treated with anti-CD29 mAb, in both Percoll-separated and MACS-separated basophils (Fig. 5*A*). No significant inhibition was observed in cells treated with anti-CD11a or anti-CD11b mAb alone, but treatment

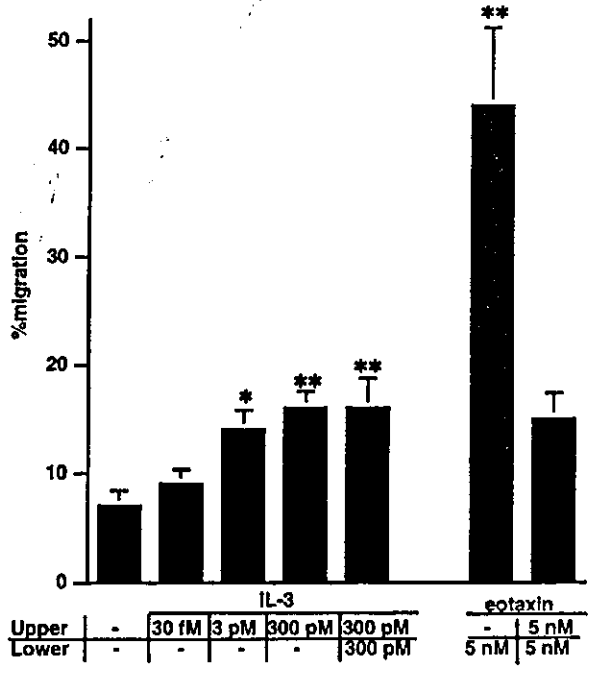

FIGURE 4. Effects of IL-3 on basophil TEM. HUVEC were treated with IL-1-β (5 ng/ml) at 37°C for 4 h. IL-3 and eotaxin (5 nM) were added to the upper and/or lower wells as indicated. Basophils were separated by Percoll, and TEM assay was performed at 37°C for 3 h. Bars represent the SEM ($n = 8$). *, $p < 0.05$; **, $p < 0.01$ (vs spontaneous migration without IL-3 or eotaxin).

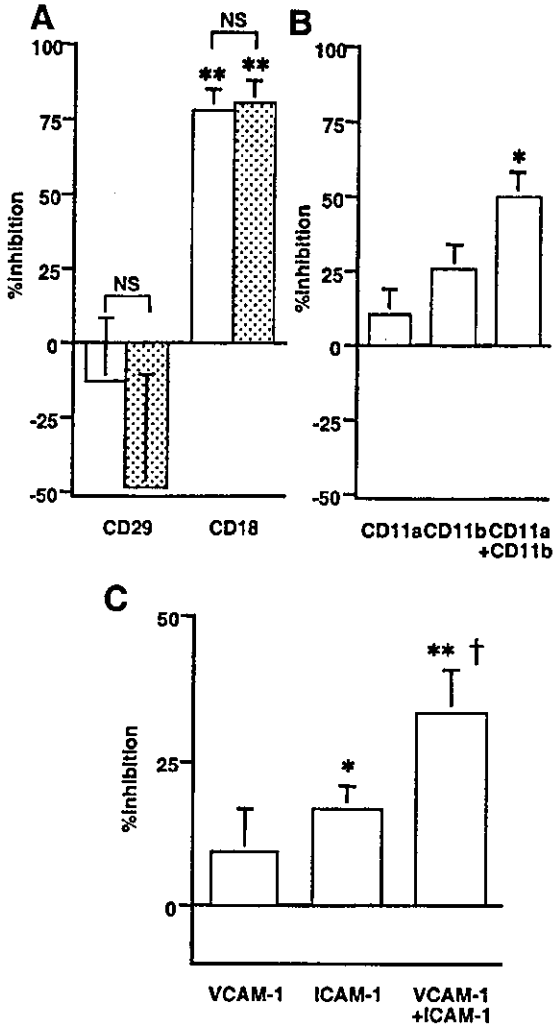

FIGURE 5. Effects of adhesion molecules on spontaneous basophil TEM across activated HUVEC. *A*, HUVEC were pretreated with IL-1-β (5 ng/ml) at 37°C for 4 h. Percoll-separated (□) and MACS-separated (□) basophils were preincubated with anti-adhesion molecule mAb (10 μg/ml) or isotype control mAb (mouse IgG1) at 37°C for 30 min. The TEM assay was performed at 37°C for 3 h. Bars represent the SEM ($n = 4$). The purities of Percoll- and MACS-separated basophils were 17.6 ± 3.7 and 98.8 ± 0.9%, respectively. Control migrations of Percoll-separated and highly purified basophils pretreated with control mAb were 4.6 ± 1.8 and 3.3 ± 1.6%, respectively. *, $p < 0.05$; **, $p < 0.01$ (vs control migration). NS, no significant difference between Percoll-separated and highly purified basophils. *B*, HUVEC were pretreated with IL-1β (5 ng/ml) at 37°C for 4 h. Percoll-separated basophils were preincubated with anti-adhesion molecule mAb (10 μg/ml) or isotype control mAb (mouse IgG1) at 37°C for 30 min. The TEM assay was performed at 37°C for 3 h. Bars represent the SEM ($n = 8$–10). Control migration of basophils pretreated with control mAb was 7.3 ± 1.1%. *, $p < 0.05$; **, $p < 0.01$ (vs control migration). *C*, IL-1-stimulated HUVEC were pretreated with the $F(ab')_2$ of anti-VCAM-1 mAb (3 μg/ml), anti-ICAM-1 mAb (10 μg/ml), or control Ab (mouse IgG, 10 μg/ml) at 37°C for 30 min. The TEM assay was performed using Percoll-separated basophils at 37°C for 3 h. Bars represent the SEM ($n = 6$). Control migration across HUVEC precultured with the $F(ab')_2$ of control Ab was 9.5 ± 1.8%. *, $p < 0.05$; **, $p < 0.01$ (vs control migration). †, $p < 0.05$ (vs migration after pretreatment with anti-ICAM-1 mAb).

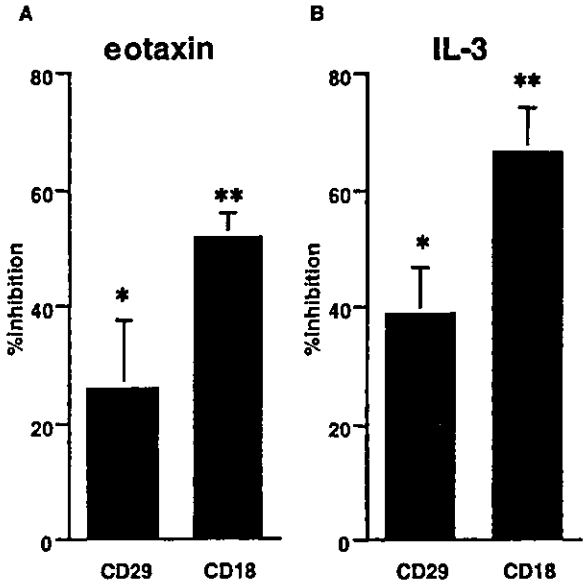

FIGURE 6. Effects of adhesion molecules on eotaxin-mediated (*A*) and IL-3-mediated (*B*) basophil TEM across activated HUVEC. HUVEC were pretreated with IL-1-β (5 ng/ml) at 37°C for 4 h. *A*, Percoll-separated basophils were treated with anti-CD18 mAb (10 μg/ml), anti-CD29 mAb (10 μg/ml), or isotype control mAb (10 μg/ml) at 37°C for 30 min. TEM assay was performed at 37°C for 3 h in the presence of eotaxin (5 nM) in the lower wells. *B*, Percoll-separated basophils were preincubated with IL-3 (300 pM) at 37°C for 30 min plus anti-CD18 mAb (10 μg/ml), anti-CD29 mAb (10 μg/ml), or isotype control mAb (10 μg/ml) at 37°C for 30 min. Basophil TEM was performed at 37°C for 3 h. Bars represent the SEM (n = 6–8). Control migrations induced by eotaxin and IL-3 in the case of basophils pretreated with isotype control mAb were 22.7 ± 7.6 and 22.4 ± 3.4%, respectively. Spontaneous TEM without eotaxin or IL-3 was 8.6 ± 1.7%. *, $p < 0.05$; **, $p < 0.01$ (vs control migration).

with a combination of both mAbs resulted in significant inhibition of basophil TEM (Fig. 5*B*). In contrast, as expected, neither anti-CD49d nor anti-CD49e mAb inhibited TEM (−14.6 ± 24.3 and −37.5 ± 26.8%, inhibitory effects of anti-CD49d and anti-CD49e mAb, respectively; n = 7). Fig. 5*C* depicts the effects of counter-receptors of endothelial cells on spontaneous TEM. When IL-1-stimulated HUVEC were pretreated with F(ab′)$_2$ of anti-CD106 (VCAM-1) or anti-CD54 (ICAM-1) mAb, we found that TEM of fresh basophils was significantly inhibited by anti-ICAM-1 mAb alone. Although anti-VCAM-1 mAb alone failed to exert a significant inhibitory effect, the combination of anti-VCAM-1 and anti-ICAM-1 mAbs produced enhanced inhibition compared with anti-ICAM-1 alone, indicating an additive inhibitory effect of anti-VCAM-1 mAb. Taken together, these results indicate that the β_2 integrin/ICAM-1 system is mainly responsible for TEM of fresh basophils across activated HUVEC, in which the β_1 integrin/VCAM-1 system may also play an additive role.

In contrast to spontaneous TEM, eotaxin-induced TEM was significantly inhibited not only by anti-CD18 mAb, but also by anti-CD29 mAb (Fig. 6*A*). The inhibition by anti-CD29 mAb was significantly less prominent than that by anti-CD18 mAb. TEM of IL-3-primed basophils was also inhibited by anti-CD29 mAb, although again less potently than with anti-CD18 mAb. These results indicate that β_1 integrins are more actively involved in eotaxin- or IL-3-induced basophil TEM, in contrast to spontaneous TEM.

Discussion

Participation of basophils in allergic inflammation has been strongly inferred from both the increase in the number of these cells and the presence of basophil-derived mediators at inflammatory sites during allergic reactions (2–6, 9). TEM represents an essential step for movement of leukocytes from the circulation to inflamed tissue sites, and numerous reports have extensively studied TEM of various types of leukocytes (26). In contrast, to our knowledge no studies have dealt with basophil TEM to date. In the present study, using well-established assay systems, for the first time we have investigated basophil migration across vascular endothelial cell monolayers.

The chemokine family has been highly implicated in the pathogenesis of inflammation of various etiologies (27). In addition, several lines of evidence have demonstrated that chemokines play an important role in TEM of various leukocytes (28–31). The same situation was observed in TEM of basophils. We previously studied the expression profile and functions of chemokine receptors in human basophils (13). CCR3 is constitutively expressed on the basophil surface, and CCR3 ligands such as eotaxin induced the most potent migratory responses in freshly isolated basophils. In contrast, although surface expression of CXCR4 is hardly detectable in freshly isolated basophils, it becomes gradually apparent during culture, and SDF-1 induces a strong migratory response, comparable to that induced by eotaxin (13). In parallel to these previous findings, our present results show the involvement of both CCR3 and CXCR4 in basophil TEM; strong TEM was induced by CCR3 ligands in freshly isolated cells and by SDF-1 in 24-h cultured basophils (Fig. 2*B*). The physiological role of CXCR4 on basophils is uncertain at present. However, as discussed in our previous paper (13), constitutive and ubiquitous expression of SDF-1 in many tissues suggests that CXCR4 is involved, rather, in baseline trafficking of basophils. In the present study we found that CCR2, which is strongly expressed on basophils (13, 16), is also actively involved in basophil TEM. Our earlier report showed that whereas CCR2 causes the most potent degranulation of basophils (13), its migration-inducing ability is only marginal. Based on the numbers of migrated basophils, MCP-1 is ~5-fold less potent than eotaxin (13). In contrast to those findings, the present study demonstrated that MCP-1 elicited strong basophil TEM, comparable to that induced by eotaxin. This observation is of potential importance, because CCR2 is virtually undetectable on human eosinophils (32), and MCP-1 fails to induce eosinophil TEM at all (29). As discussed below, many of the regulatory mechanisms of TEM of basophils are shared with eosinophils. Therefore, MCP-1-mediated basophil TEM may represent a unique mechanism for selective migration of human basophils. In contrast, we failed to observe any significant direct effects of CCR1, CCR2, CCR5, CXCR1, and CXCR2 on basophil TEM. Thus, although we cannot exclude possible additional effects of these receptors, it is reasonably concluded that basophil TEM is regulated mainly by both CCR2 and CCR3, and by CXCR4 under certain circumstances.

HUVEC are capable of liberating various chemokines in response to diverse stimuli (33–35). Therefore, it should be noted that HUVEC-derived chemokines might disturb the chemotactic gradient and thereby affect the TEM results. Furthermore, more complicated mechanisms may exist regarding the CXCR4/SDF-1 system; Murdoch et al. (36) reported that HUVEC expressed CXCR4 and induced a rapid calcium influx in response to SDF-1. Inasmuch as CXCR4 on vascular endothelial cells is up-regulated by activating stimuli, the presence of SDF-1 may induce and/or modulate cytokine/chemokine production by activated HUVEC. Even though we stimulated HUVEC for only a short time (4 h) and eliminated possible soluble factors from HUVEC by washing before performing TEM assays, there remains the possibility that HUVEC-derived mediators might affect the TEM results, as reported for eosinophil TEM (34).

We and others have demonstrated that IL-3 represents the most potent basophil-activating cytokine and stimulates various aspects of basophil functions, including mediator release (21, 22), survival (23, 24), motility (11), adhesiveness to the endothelium (14), and expression of activation markers (14). Our present finding that IL-3 potentiated basophil TEM broadens the current concept of the capacity of IL-3 to modulate allergic inflammatory responses by up-regulating basophil functions. However, it seems unlikely that IL-3 is directly involved in basophil accumulation at allergic inflammatory sites, because checkerboard analyses clearly showed that IL-3-mediated TEM was chemokinetic rather than chemotactic. Nevertheless, the additive effect of IL-3 seen in eotaxin-induced TEM strongly suggested that IL-3, and potentially IL-5 and GM-CSF as well, plays a cooperative role in basophil TEM with these basophil-directed chemokines by modulating locomotive movement.

In addition to basophil-directed cytokines and chemokines, adhesion molecules play a critical role in basophil TEM. Although basophils express both β_1 and β_2 integrins (12), we found that β_2 integrins represent the first line of adhesion molecules that account for basophil TEM. TEM of fresh basophils across activated HUVEC was significantly attenuated by treatment with anti-CD18 mAb. Cotreatment with anti-CD11a and anti-CD11b mAbs showed additive inhibitory effects, indicating the involvement of both the α_L and α_M chains in basophil TEM. In line with these observations, pretreatment of activated HUVEC with mAb against ICAM-1, a counter-receptor for both CD11a and CD11b, significantly inhibited basophil TEM. Furthermore, basophil TEM induced by IL-3 or eotaxin was also suppressed by anti-CD18 mAb. An in vitro study by others showed up-regulation of the expression of a β_2 integrin (CD11b) by IL-3 (14). We found that CD11b and CD18 were also up-regulated by IL-3, and that eotaxin exerted the same effect to a lesser extent (M. Iikura and K. Hirai, unpublished observation). Thus, the enhanced TEM observed in IL-3- and eotaxin-treated cells can be attributed at least in part to strengthened interaction with β_2 integrin caused by up-regulated expression of these molecules.

Our results indicated an additional role of β_1 integrins in basophil TEM. Spontaneous TEM across activated HUVEC was not inhibited by anti-CD49d, anti-49e, or anti-CD29 mAb (Fig. 5*A*), but anti-CD29 mAb significantly inhibited TEM of eotaxin- and IL-3-stimulated basophils (Fig. 6). The increase in the involvement of β_1 integrin in these cells is potentially mediated by functional up-regulation of β_1 integrin. Sung et al. (37) reported that short term incubation of eosinophils with eotaxin or GM-CSF (30 min) up-regulates the binding of cells to VCAM-1 without affecting the expression level of VLA-4 protein. Although not proven, a conformational change in the VLA-4 receptor is likely to be responsible for the increased involvement of β_1 integrin in basophils stimulated with either eotaxin or IL-3. Because β_1 integrin is specifically expressed on basophils and eosinophils, but not neutrophils (38), this molecule is strongly implicated in the selective accumulation of basophils as well as eosinophils at allergic inflammatory sites.

The results of blocking experiments showed a discrepancy in the efficacy between inhibition of α and β subunits as well as counter-receptors and leukocyte integrins. This discrepancy strongly suggests additional involvement of untested adhesion molecules in basophil TEM. Although our present results indicated essential roles for α_L and α_M in basophil TEM, the blockade of the β subunit (CD18) was more effective than that of a combination of CD11a plus CD11b (Fig. 5, *A* and *B*). The lower efficacy of blockade of α subunits indicates possible roles for other members of α subunits of β_2 integrin, i.e., CD11c (α_X) and α_d, which have been shown to be constitutively expressed on basophils (39, 40). A similar situation was postulated for counter-receptors of Ig superfamily members. We found that anti-VCAM-1 mAb showed an additive inhibitory effect in combination with anti-ICAM-1 mAb on TEM of fresh basophils regardless of the inefficacy of anti-CD29 treatment (Fig. 5, *A* and *C*). Because $\alpha_d\beta_2$ integrins use VCAM-1 as one of their counter-receptors (41), an additive role for VCAM-1 may also support the involvement of $\alpha_d\beta_2$ integrins in spontaneous basophil TEM. Furthermore, our finding that blockade of counter-receptors is markedly less effective than that of leukocyte integrins (Fig. 5, *A* and *C*) may reflect the involvement of other untested Ig superfamily members, such as ICAM-2. Additional study is required to elucidate the possible roles of these molecules in basophil TEM.

The increased TEM observed in IL-1-stimulated HUVEC indicated the importance of endothelial cell activation in basophil TEM. Throughout our experiments we used HUVEC stimulated with IL-1β for 4 h, which up-regulates mainly ICAM-1 expression (42). However, the expression profile of counter-receptors on endothelial cells varies in a stimulus- and time-dependent fashion. Furthermore, phenotypic and functional heterogeneity of vascular endothelial cells is observed among different tissues. For example, IL-4 selectively induces VCAM-1 expression in HUVEC (43) or nasal polyp-derived microvascular endothelium (44), but not in microvascular endothelial cells from skin (45), intestine (46), or lung (47). In contrast, VCAM-1 expression of pulmonary microvascular endothelial cells was selectively up-regulated by long term (24-h) stimulation with TNF-α (47). Thus, it is highly likely that basophil TEM across endothelial cells obtained from other organs and/or stimulated with other cytokines would show a different profile from our present results derived using IL-1-activated HUVEC. To elucidate the precise mechanisms of basophil TEM in various allergic diseases, basophil TEM across these endothelial cells is an important issue meriting additional investigation.

Substantial evidence to date has clearly indicated a close relationship between basophils and eosinophils (48). Both cell types share a majority of their cell surface structures, including cytokine/chemokine receptors and adhesion molecules. The activating hemopoietins for both cells, i.e., IL-3, GM-CSF, and IL-5, completely overlap, and CCR3 induces strong migratory responses of basophils as well as eosinophils. Furthermore, in contrast to neutrophils, β_1 integrins in addition to β_2 integrins are specifically expressed on the surface of both cells. The results of the present study clearly show that the regulatory profile of basophil TEM is very similar to that reported for eosinophils (19, 29, 31, 49, 50). In addition to regulatory cytokines and chemokines, adhesion molecules are also involved in TEM of basophils in a quite similar fashion as in TEM of eosinophils. These common aspects of TEM determined in vitro strongly suggest similarity of the in vivo kinetics of these two cell types.

In summary, for the first time we have studied the profile and regulation of basophil TEM using IL-1-activated HUVEC. Basophil-activating hemopoietin IL-3 and basophil-directed chemokines, such as CCR2 and CCR3 ligands, are critically involved in TEM of basophils. Although β_2 integrin/ICAM-1 plays a major role in basophil TEM, β_1 integrin/VCAM-1 clearly plays an additional role. These profiles of the regulation of basophil TEM are very similar to those of eosinophil TEM, except for that by CCR2 ligand MCP-1. Our results thus support the previous argument for a close relationship between basophils and eosinophils, and suggest similar in vivo kinetics for these two cell types.

Acknowledgments

We thank M. Imanishi and C. Tamura for their skilled technical assistance. Thanks are also extended to S. Takeyama for her excellent secretarial help.

References

1. Schroeder, J. T., D. W. MacGlashan, Jr., and L. M. Lichtenstein. 2001. Human basophils: mediator release and cytokine production. *Adv. Immunol. 77:93.*
2. Naclerio, R. M., D. Proud, A. G. Togias, N. F. Adkinson, Jr., D. A. Meyers, A. Kagey-Sobotka, M. Plaut, P. S. Norman, and L. M. Lichtenstein. 1985. Inflammatory mediators in late antigen-induced rhinitis. *N. Engl. J. Med. 313:65.*
3. Charlesworth, E. N., A. F. Hood, N. A. Soter, A. Kagey-Sobotka, P. S. Norman, and L. M. Lichtenstein. 1989. Cutaneous late-phase response to allergen: mediator release and inflammatory cell infiltration. *J. Clin. Invest. 83:1519.*
4. Lichtenstein, L. M., and B. S. Bochner. 1991. The role of basophils in asthma. *Ann. NY Acad. Sci. 629:48.*
5. Iliopoulos, O., F. M. Baroody, R. M. Naclerio, B. S. Bochner, A. Kagey-Sobotka, and L. M. Lichtenstein. 1992. Histamine-containing cells obtained from the nose hours after antigen challenge have functional and phenotypic characteristics of basophils. *J. Immunol. 148:2223.*
6. Guo, C. B., M. C. Liu, S. J. Galli, B. S. Bochner, A. Kagey-Sobotka, and L. M. Lichtenstein. 1994. Identification of IgE-bearing cells in the late-phase response to antigen in the lung as basophils. *Am. J. Respir. Cell Mol. Biol. 10:384.*
7. Irani, A. M., C. Huang, H. Z. Xia, C. Kepley, A. Nafie, E. D. Fouda, S. Craig, B. Zweiman, and L. B. Schwartz. 1998. Immunohistochemical detection of human basophils in late-phase skin reactions. *J. Allergy Clin. Immunol. 101:354.*
8. Ying, S., D. S. Robinson, Q. Meng, L. T. Barata, A. R. McEuen, M. G. Buckley, A. F. Walls, P. W. Askenase, and A. B. Kay. 1999. C-C chemokines in allergen-induced late-phase cutaneous responses in atopic subjects: association of eotaxin with early 6-hour eosinophils, and of eotaxin-2 and monocyte chemoattractant protein-4 with the later 24-hour tissue eosinophilia, and relationship to basophils and other C-C chemokines (monocyte chemoattractant protein-3 and RANTES). *J. Immunol. 163:3976.*
9. Gauvreau, G. M., J. M. Lee, R. M. Watson, A. M. Irani, L. B. Schwartz, and P. M. O'Byrne. 2000. Increased numbers of both airway basophils and mast cells in sputum after allergen inhalation challenge of atopic asthmatics. *Am. J. Respir. Crit. Care Med. 161:1473.*
10. Bochner, B. S., P. T. Peachell, K. E. Brown, and R. P. Schleimer. 1988. Adherence of human basophils to cultured umbilical vein endothelial cells. *J. Clin. Invest. 81:1355.*
11. Yamaguchi, M., K. Hirai, S. Shoji, T. Takaishi, K. Ohta, Y. Morita, S. Suzuki, and K. Ito. 1992. Haemopoietic growth factors induce human basophil migration in vitro. *Clin. Exp. Allergy 22:379.*
12. Bochner, B. S., S. A. Sterbinsky, M. Briskin, S. S. Saini, and D. W. MacGlashan, Jr. 1996. Counter-receptors on human basophils for endothelial cell adhesion molecules. *J. Immunol. 157:844.*
13. Iikura, M., M. Miyamasu, M. Yamaguchi, H. Kawasaki, K. Matsushima, M. Kitaura, Y. Morita, O. Yoshie, K. Yamamoto, and K. Hirai. 2001. Chemokine receptors in human basophils: inducible expression of functional CXCR4. *J. Leukocyte Biol. 70:113.*
14. Bochner, B. S., A. A. McKelvey, S. A. Sterbinsky, J. E. Hildreth, C. P. Derse, D. A. Klunk, L. M. Lichtenstein, and R. P. Schleimer. 1990. IL-3 augments adhesiveness for endothelium and CD11b expression in human basophils but not neutrophils. *J. Immunol. 145:1832.*
15. Yamada, H., K. Hirai, M. Miyamasu, M. Iikura, Y. Misaki, S. Shoji, T. Takaishi, T. Kasahara, Y. Morita, and K. Ito. 1997. Eotaxin is a potent chemotaxin for human basophils. *Biochem. Biophys. Res. Commun. 231:365.*
16. Uguccioni, M., C. R. Mackay, B. Ochensberger, P. Loetscher, S. Rhis, G. J. LaRosa, P. Rao, P. D. Ponath, M. Baggiolini, and C. A. Dahinden. 1997. High expression of the chemokine receptor CCR3 in human blood basophils: role in activation by eotaxin, MCP-4, and other chemokines. *J. Clin. Invest. 100:1137.*
17. Sato, K., H. Kawasaki, H. Nagayama, R. Serizawa, J. Ikeda, C. Morimoto, K. Yasunaga, N. Yamaji, K. Tadokoro, T. Juji, et al. 1999. CC chemokine receptors, CCR-1 and CCR-3, are potentially involved in antigen-presenting cell function of human peripheral blood monocyte-derived dendritic cells. *Blood 93:34.*
18. Iikura, M., M. Yamaguchi, T. Fujisawa, M. Miyamasu, T. Takaishi, Y. Morita, T. Iwase, I. More, K. Yamamoto, and K. Hirai. 1998. Secretory IgA induces degranulation of IL-3-primed basophils. *J. Immunol. 161:1510.*
19. Ebisawa, M., B. S. Bochner, S. N. Georas, and R. P. Schleimer. 1992. Eosinophil transendothelial migration induced by cytokines. I. Role of endothelial and eosinophil adhesion molecules in IL-1β-induced transendothelial migration. *J. Immunol. 149:4021.*
20. Ochensberger, B., L. Tassera, D. Bifrare, S. Rihs, and C. A. Dahinden. 1999. Regulation of cytokine expression and leukotriene formation in human basophils by growth factors, chemokines and chemotactic agonists. *Eur. J. Immunol. 29:11.*
21. Hirai, K., Y. Morita, Y. Misaki, K. Ohta, T. Takaishi, S. Suzuki, K. Motoyoshi, and T. Miyamoto. 1988. Modulation of human basophil histamine release by hemopoietic growth factors. *J. Immunol. 141:3958.*
22. Kurimoto, Y., A. L. de Week, and C. A. Dahinden. 1989. Interleukin 3-dependent mediator release in basophils triggered by C5a. *J. Exp. Med. 170:467.*
23. Yamaguchi, M., K. Hirai, Y. Morita, T. Takaishi, K. Ohta, S. Suzuki, K. Motoyoshi, O. Kawanami, and K. Ito. 1992. Hemopoietic growth factors regulate the survival of human basophils in vitro. *Int. Arch. Allergy Immunol. 97:322.*
24. Miura, K., S. S. Saini, G. Gauvreau, and D. W. MacGlashan, Jr. 2001. Differences in functional consequences and signal transduction induced by IL-3, IL-5, and nerve growth factor in human basophils. *J. Immunol. 167:2282.*
25. Fureder, W., H. Agis, W. R. Sperr, K. Lechner, and P. Valent. 1994. The surface membrane antigen phenotype of human blood basophils. *Allergy 49:861.*
26. Luscinskas, F. W., S. Ma, A. Nusrat, C. A. Parkos, and S. K. Shaw. 2002. Leukocyte transendothelial migration: a junctional affair. *Semin. Immunol. 14:105.*
27. Gerard, C., and B. J. Rollins. 2001. Chemokines and disease. *Nat. Immunol. 2:108.*
28. Smith, W. B., J. R. Gamble, I. Clark-Lewis, and M. A. Vadas. 1991. Interleukin-8 induces neutrophil transendothelial migration. *Immunology 72:65.*
29. Ebisawa, M., T. Yamada, C. Bickel, D. Klunk, and R. P. Schleimer. 1994. Eosinophil transendothelial migration induced by cytokines. III. Effect of the chemokine RANTES. *J. Immunol. 153:2153.*
30. Randolph, G. J., and M. B. Furie. 1995. A soluble gradient of endogenous monocyte chemoattractant protein-1 promotes the transendothelial migration of monocytes in vitro. *J. Immunol. 155:3610.*
31. Shahabuddin, S., P. Ponath, and R. P. Schleimer. 2000. Migration of eosinophils across endothelial cell monolayers: interactions among IL-5, endothelial-activating cytokines, and C-C chemokines. *J. Immunol. 164:3847.*
32. Nagase, H., M. Miyamasu, M. Yamaguchi, T. Fujisawa, K. Ohta, K. Yamamoto, Y. Morita, and K. Hirai. 2000. Expression of CXCR4 in eosinophils: functional analyses and cytokine-mediated regulation. *J. Immunol. 164:5935.*
33. Miyamasu, M., T. Nakajima, Y. Misaki, S. Izumi, N. Tsuno, T. Kasahara, K. Yamamoto, Y. Morita, and K. Hirai. 1999. Dermal fibroblasts represent a potent major source of human eotaxin: in vitro production and cytokine-mediated regulation. *Cytokine 11:751.*
34. Cuvelier, S. L., and K. D. Patel. 2001. Shear-dependent eosinophil transmigration on interleukin 4-stimulated endothelial cells: a role for endothelium-associated eotaxin-3. *J. Exp. Med. 194:1699.*
35. Komiya, A., H. Nagase, H. Yamada, T. Sekiya, M. Yamaguchi, Y. Sano, N. Hanai, A. Furuya, K. Ohta, K. Matsushima, et al. 2003. Concerted expression of eotaxin-1, eotaxin-2, and eotaxin-3 in human bronchial epithelial cells. *Cell. Immunol. 225:91.*
36. Murdoch, C., P. N. Monk, and A. Finn. 1999. Cxc chemokine receptor expression on human endothelial cells. *Cytokine 11:704.*
37. Sung, K. P., L. Yang, J. Kim, D. Ko, G. Stachnick, D. Castaneda, J. Nayar, and D. H. Broide. 2000. Eotaxin induces a sustained reduction in the functional adhesive state of very late antigen 4 for the connecting segment 1 region of fibronectin. *J. Allergy Clin. Immunol. 106:933.*
38. Bochner, B. S., F. W. Luscinskas, M. A. Gimbrone, Jr., W. Newman, S. A. Sterbinsky, C. P. Derse-Anthony, D. Klunk, and R. P. Schleimer. 1991. Adhesion of human basophils, eosinophils, and neutrophils to interleukin 1-activated human vascular endothelial cells: contributions of endothelial cell adhesion molecules. *J. Exp. Med. 173:1553.*
39. Bochner, B. S., and S. A. Sterbinsky. 1991. Altered surface expression of CD11 and Leu 8 during human basophil degranulation. *J. Immunol. 146:2367.*
40. Grayson, M. H., M. Van der Vieren, W. M. Gallatin, P. A. Hoffman, and B. S. Bochner. 1997. Expression of a novel β_2 integrin ($\alpha_d\beta_2$) on human leukocytes and mast cells. *J. Allergy Clin. Immunol. 99:S386.*
41. Grayson, M. H., M. Van der Vieren, S. A. Sterbinsky, W. M. Gallatin, P. A. Hoffman, D. E. Staunton, and B. S. Bochner. 1998. $\alpha_d\beta_2$ integrin is expressed on human eosinophils and functions as an alternative ligand for vascular cell adhesion molecule 1 (VCAM-1). *J. Exp. Med. 188:2187.*
42. Bochner, B. S., D. A. Klunk, S. A. Sterbinsky, R. L. Coffman, and R. P. Schleimer. 1995. IL-13 selectively induces vascular cell adhesion molecule-1 expression in human endothelial cells. *J. Immunol. 154:799.*
43. Schleimer, R. P., S. A. Sterbinsky, J. Kaiser C. A. Bickel, D. A. Klunk, K. Tomioka, W. Newman, F. W. Luscinskas, M. A. Gimbrone, Jr., B. W. McIntyre, et al. 1992. IL-4 induces adherence of human eosinophils and basophils but not neutrophils to endothelium: association with expression of VCAM-1. *J. Immunol. 148:1086.*
44. Jahnsen, F. L., P. Brandtzaeg, R. Haye, and G. Haraldsen. 1997. Expression of functional VCAM-1 by cultured nasal polyp-derived microvascular endothelium. *Am. J. Pathol. 150:2113.*
45. Swerlick, R. A., K. H. Lee, L. J. Li, N. T. Sepp, S. W. Caughman, and T. J. Lawley. 1992. Regulation of vascular cell adhesion molecule 1 on human dermal microvascular endothelial cells. *J. Immunol. 149:698.*
46. Haraldsen, G., D. Kvale, B. Lien, I. N. Farstad and P. Brandtzaeg. 1996. Cytokine-regulated expression of E-selectin, intercellular adhesion molecule-1 (ICAM-1), and vascular cell adhesion molecule-1 (VCAM-1) in human microvascular endothelial cells. *J. Immunol. 156:2558.*
47. Yamamoto, H., J. B. Sedgwick, and W. W. Busse. 1998. Differential regulation of eosinophil adhesion and transmigration by pulmonary microvascular endothelial cells. *J. Immunol. 161:971.*
48. Hirai, K., M. Miyamasu, T. Takaishi, and Y. Morita 1997. Regulation of the function of eosinophils and basophils. *Crit. Rev. Immunol. 17:325.*
49. Ebisawa, M., M. C. Liu, T. Yamada, M. Kato, L. M. Lichtenstein, B. S. Bochner, and R. P. Schleimer. 1994. Eosinophil transendothelial migration induced by cytokines. II. Potentiation of eosinophil transendothelial migration by eosinophil-active cytokines. *J. Immunol. 152:4590.*
50. Jia, G. Q., J. A. Gonzalo, A. Hidalgo, D. Wagner, M. Cybulsky, and J. C. Gutierrez-Ramos. 1999. Selective eosinophil transendothelial migration triggered by eotaxin via modulation of Mac-1/ICAM-1 and VLA-4/VCAM-1 interactions. *Int. Immunol. 11:1.*

Nucleosome-Specific Regulatory T Cells Engineered by Triple Gene Transfer Suppress a Systemic Autoimmune Disease[1]

Keishi Fujio,* Akiko Okamoto,* Hiroyuki Tahara,* Masaaki Abe,† Yi Jiang, † Toshio Kitamura,‡ Sachiko Hirose,† and Kazuhiko Yamamoto[2]*

The mechanisms of systemic autoimmune disease are poorly understood and available therapies often lead to immunosuppressive conditions. We describe here a new model of autoantigen-specific immunotherapy based on the sites of autoantigen presentation in systemic autoimmune disease. Nucleosomes are one of the well-characterized autoantigens. We found relative splenic localization of the stimulative capacity for nucleosome-specific T cells in (NZB × NZW)F_1 (NZB/W F_1) lupus-prone mice. Splenic dendritic cells (DCs) from NZB/W F_1 mice spontaneously stimulate nucleosome-specific T cells to a much greater degree than both DCs from normal mice and DCs from the lymph nodes of NZB/W F_1 mice. This leads to a strategy for the local delivery of therapeutic molecules using autoantigen-specific T cells. Nucleosome-specific regulatory T cells engineered by triple gene transfer (TCR-α, TCR-β, and CTLA4Ig) accumulated in the spleen and suppressed the related pathogenic autoantibody production. Nephritis was drastically suppressed without impairing the T cell-dependent humoral immune responses. Thus, autoantigen-specific regulatory T cells engineered by multiple gene transfer is a promising strategy for treating autoimmune diseases. ***The Journal of Immunology,*** **2004, 173: 2118–2125.**

Systemic autoimmune diseases have traditionally been treated using nonspecific immunosuppressive agents, but these agents often lead to opportunistic infections and an increased rate of malignancy. There remains the need to develop selective or specific therapies that target individual autoantigens. Several strategies have been developed as potential Ag-specific immunotherapies, such as using Ag-pulsed dendritic cells (DCs),[3] but the majority of these approaches will require further investigation (1, 2). A more detailed understanding of autoimmune diseases, including autoantigen presentation, is required for the development of reasonable immunotherapies.

Systemic lupus erythematosus (SLE) is a life-threatening autoimmune disease characterized by the production of a variety of autoantibodies (3). Anti-DNA Abs are thought to be one of the major pathogenic products of the autoimmune response (4–6). Datta and colleagues (7–9), as well as other groups (10, 11), have noted that nucleosomes could be a major immunogen for pathogenic autoantibody-inducing T cells in lupus-prone mice. Datta and coworkers (7–9) showed that the majority of pathogenic T_H clones specific for nucleosomes were capable of rapidly inducing anti-DNA autoantibody production, and that these clones were also able to induce nephritis when injected into young lupus-prone mice. Moreover, anti-nucleosome ELISAs have demonstrated better sensitivity, specificity, and diagnostic confidence with regard to human SLE than anti-DNA ELISAs. Anti-nucleosome ELISAs are also correlated with disease activity, as determined by the SLE Disease Activity Index (12, 13).

Although evidences have accumulated demonstrating the importance of nucleosomes as major pathogenic autoantigens, the cellular mechanisms for the immunological recognition of nucleosomes are poorly understood. Generalized hyperresponsiveness of B cells has been reported in both mice and human lupus (14, 15). However, these nonspecific immune disorders cannot provide a sufficient model of nuclear autoantigen-specific autoimmunity encountered in patients with lupus.

To better understand the mechanisms of autoantigen recognition, we first reconstituted nucleosome specificity by TCR gene transfer in $CD4^+$ T cells from (NZB × NZW)F_1 (NZB/W F_1) lupus model mice (3, 16). Using this model, we demonstrated an abnormal autoantigen presentation of splenic DCs. Among the lymphoid organs, this elevated autoantigen presentation of DCs was relatively localized in the spleen. We then developed a triple gene transfer system to generate autoantigen-specific regulatory cells. These regulatory cells preferentially accumulated in the spleen and suppressed the progression of the disease without obvious systemic immunosuppression.

Materials and Methods

Preparation of retroviral construct

Line 3A is a cell line from lupus-prone (SWR × NZB)F_1 (SNF1; I-$A^{d/q}$) that can recognize the immunodominant nucleosomal epitope (histone H4; aa 71–94) in the context of I-A^d (7, 8) and many other I-A molecules (8). Both TCR-α and -β cDNA fragments were synthesized using PCR based on the published sequences of line 3A (7, 8) and designated as AN3 TCR-α and -β. Vα13 and Vβ4 fragments identical to CDR1 and two sequences of line 3A were obtained from NZB splenic cDNA and an added CDR3 sequence by PCR. Jα41-Cα fragment and Jβ2.6-Cβ fragment were also obtained from NZB splenic cDNA and an added CDR3 sequence by PCR. Vα13-CDR3 fragment and CDR3-Jα41-Cα fragment were combined in a

*Department of Allergy and Rheumatology, Graduate School of Medicine, University of Tokyo, Tokyo, Japan; †Department of Pathology, Juntendo University School of Medicine, Tokyo, Japan; and ‡Division of Cellular Therapy, Advanced Clinical Research Center, Institute of Medical Science, University of Tokyo, Tokyo, Japan

Received for publication September 24, 2003. Accepted for publication May 12, 2004.

The costs of publication of this article were defrayed in part by the payment of page charges. This article must therefore be hereby marked *advertisement* in accordance with 18 U.S.C. Section 1734 solely to indicate this fact.

[1] This study was supported by grants from the Ministry of Health, Labor and Welfare and the Ministry of Education, Culture, Sports, Science and Technology of Japan.

[2] Address correspondence and reprint requests to Dr. Kazuhiko Yamamoto, Department of Allergy and Rheumatology, Graduate School of Medicine, University of Tokyo, 7-3-1 Hongo, Bunkyo-ku, Tokyo, 113-0033, Japan. E-mail address: yamamoto-tky@umin.ac.jp

[3] Abbreviations used in this paper: DC, dendritic cell; SLE, systemic lupus erythematosus; WPRE, woodchuck hepatitis virus posttranscriptional regulatory element; IRES, internal ribosomal entry site; LN, lymph node.

0022-1767/04/$02.00

subsequent "fusion" reaction in which the overlapping ends anneal, allowing the 3′ overlap of each strand to serve as a primer for the 3′ extension of the complementary strand. The resulting fusion product is amplified further by PCR. Vβ4-CDR3 fragment and CDR3-Jβ2.6-Cβ fragment were combined similarly. The full-length fragments were cloned into a pMXW retroviral vector to obtain pMXW-AN3α and pMXW-AN3β (Fig. 1*A*). pMXW is an improved vector generated by insertion of the woodchuck hepatitis virus posttranscriptional regulatory element (WPRE) (17, 18) between the *NotI* and *SalI* sites of pMX (19). WPRE enhances expression of transgenes delivered by retroviral vectors (18), and the expression efficiency of the pMXW vector is improved 1.5 times when WPRE is inserted, compared with the efficiency of the pMX vector. Murine CTLA4Ig cDNA was synthesized by PCR as described previously (20) and was then cloned into the pMX-IRES-GFP (21). Complementary DNAs for the TCR α- and β-chains were isolated from a cDNA library of DO11.10 TCR-transgenic splenocytes and were inserted into the retroviral vector pMX to generate pMX-DOTAE and pMX-DOTBE, respectively (22).

Mice

NZB/W F_1 and BALB/c mice were obtained from Japan SLC (Shizuoka, Japan). All animal experiments were conducted in accordance with the institutional and national guidelines.

Production of retroviral supernatants and retroviral transduction

Total splenocytes were isolated and cultured for 48 h in RPMI 1640 medium supplemented with 10% FCS, 2 mM L-glutamine, 100 U/ml penicillin, 100 μg/ml streptomycin, and 5×10^{-5} M 2-ME in the presence of Con A (10 μg/ml) and IL-2 (50 ng/ml) before the transduction. Retroviral supernatants were obtained by transfection of pMXW, pMXW-AN3α, pMXW-AN3β, pMX-IRES-GFP, pMX-CTLA4Ig-IRES-GFP, pMX-DOTAE, or pMX-DOTBE DNA into PLAT-E packaging cell lines (22, 23) with the use of the FuGENE 6 transfection reagent (Roche Diagnostic Systems, Somerville, NJ).

Falcon 24-well plates (BD Biosciences, San Jose, CA) were coated with the recombinant human fibronectin fragment CH296 (Retronectin; Takara, Otsu, Japan) according to the manufacturer's instructions. Before infection, virus-bound plates were prepared. The viral supernatant (500 μl) was preloaded onto each well of the CH296-coated plate, and the plate was spun at 2000 × *g* for 3 h at 32°C. The virus-coating procedure was repeated three times. Before infection, the viral supernatant was washed away and splenocytes prestimulated for 48 h were added to each well (1×10^6 cells/well). Cells were cultured for 36 h to allow infection to occur. To control the viral expression efficiency, we produced a viral supernatant (pMXW, pMXW-AN3α, pMXW-AN3β, pMX-IRES-GFP, and pMX-CTLA4Ig-IRES-GFP, simultaneously) and prechecked the uniformity of the infection efficiency before in vitro and in vivo experiments.

Cell purification

A $CD4^+$ T cell population was prepared by negative selection with MACS using anti-CD19 mAb, anti-CD11c, mAb, and anti-CD8a mAb. $CD11c^+$ DCs were prepared as previously described (24, 25). Briefly, spleen cells or lymph node cells were digested with collagenase type IV (Sigma-Aldrich, St. Louis, MO) and DNase I, and the $CD11c^+$ cells were selected twice by positive selection using MACS CD11c microbeads and magnetic separation columns. The purity (85% in average) was determined by visualization with anti-CD11c-biotin followed by streptavidin-PE. A $CD19^+$ B cell population was prepared by positive selection with MACS using anti-CD19 mAb. For CFSE labeling (Molecular Probes, Eugene, OR), cells were resuspended in PBS at 1×10^7/ml and incubated with CFSE at a final concentration of 5 mM for 30 min at 37°C, followed by two washes in PBS.

Nucleosome preparation

Pure nucleosomes were prepared as previously described (26). Briefly, frozen pure chicken erythrocytes were thawed and suspended in lysis buffer on ice (10 mM Tris-HCl, 10 mM NaCl, 5 mM $MgCl_2$, 0.5% Nonidet P-40, and 0.25 mM $PhMeSO_2F$, pH 7.5). The nuclei were recovered by centrifugation and the nuclear pellet was washed and digested with micrococcal nuclease. The nuclear pellet was lysed into 0.2 mM Na_2EDTA, and nuclear debris was removed by centrifugation. The soluble chromatin at $A_{260} \approx 100$ was dialyzed against 5 mM triethanolamine HCl, 60 mM NaCl, 1 mM Na_2EDTA (pH 7.5), and subsequently fractionated in the same buffer, usually in sucrose gradients. Gradients were fractionated and monitored at 280 nm, and the appropriate fractions were pooled.

Proliferation assay

At 24 h postinfection, purified $CD4^+$ T cells were cultured at 2×10^4cells/well, with 1×10^5 cells/well of irradiated $CD19^+$ B cells or 1×10^4 cells/well of irradiated $CD11c^+$ DCs in 96-well flat-bottom microtiter plates in volumes of 100 μl of complete medium with or without 1 μg/ml nucleosome or 0.3 μM chicken $OVA_{323-339}$ peptide. After 24 h of culture, the cells were pulse labeled with 1 μCi of [^{3}H]thymidine/well (NEN Life Science Products, Boston, MA) for 15 h and the [^{3}H]thymidine incorporation was determined. In some experiments, we calculated the ratio of (group A − cpm)/(group B − cpm) in each experiment and showed the average ratio of three to five experiments as "average ratio of (group A − cpm)/(group B − cpm) to clarify the reproducibility of the data.

Transfer experiments

The indicated number of cells suspended in PBS were i.v. injected into mice. For the transfer of gene-transduced cells, cell viability was always >97%, as detected by trypan blue exclusion.

ELISA

IgG anti-DNA Abs were quantified using ELISA plates coated with calf thymus DNA (Sigma-Aldrich, and the DNA-binding activities were expressed in units, referring to a standard curve obtained by serial dilutions of a standard serum pool from 7- to 9-mo-old NZB/W F_1 mice, containing 1000 U/ml. IgG antinucleosome Abs or IgG anti-histone Abs were quantified using ELISA plates coated with purified nucleosome or purified histone. Methods for detection of CTLA4Ig protein were described previously (27). Briefly, ELISA plates were coated with anti-mouse CTLA4 (BD PharMingen, San Diego, CA) overnight at 4°C, blocked with blocking solution, and then incubated sequentially for 1 h at 37°°C with serial dilutions of serum or culture supernatants followed by peroxidase-conjugated $F(ab')_2$ goat anti-mouse IgG2a (Accurate Antibodies, Westbury, NY) and ABTS substrate (Kirkegaard & Perry, Gaithersburg, MD). Serial dilutions of a known concentration of purified CTLA4Ig were used in each plate to establish a standard curve.

Histopathology

Organs were fixed in 4% paraformaldehyde, embedded in paraffin, and stained with periodic acid-Schiff solution. For three-color immunofluorescence staining, sections were incubated with biotinylated peanut agglutinin (Vector Laboratories, Burlingame, CA) and then with Cy5.5-conjugated streptavidin (Cortex Biochemicals, Irvine, CA). The sections were then stained with a rat Alexa488-labeled mAb to B220 and tetramethylrhodamine-conjugated mAbs to CD4 and CD8 (Vector Laboratories). To detect the deposition of immune complexes at glomeruli, we incubated sections with FITC-labeled goat Abs to mouse IgG or to C3 (ICN Pharmaceuticals, Costa Mesa, CA).

Statistical analysis

Statistical significance was determined using the unpaired Student's *t* test or the Mann-Whitney *U* test.

Results

Transduction of nucleosome-specific AN3 TCR confers specificity for the nucleosome and autoreactivity to DCs in NZB/W F_1 $CD4^+$ T cells

We previously reported successful TCR gene transfer and reconstitution of the Ag specificity to OVA in BALB/c $CD4^+$ T cells (27). In the present study, we transferred nucleosome-specific TCR genes (AN3α and β) into NZB/W F_1 splenocytes. To improve the expression of the introduced genes, we generated a Moloney-based retroviral vector, pMXW, by insertion of the woodchuck fragment (17, 18) into pMX (19). We selected the TCR of line 3A from lupus-prone SNF1 mice. A hybridoma transfected with this TCR did not exhibit any significant response to either $H\text{-}2^d$ or $H\text{-}2^z$ APCs (28). Each TCR gene was inserted into pMXW, and the resulting retrovirus vectors (pMXW-AN3α and pMXW-AN3β) were used for the gene transfer (Fig. 1*A*).

Retroviral infection of the AN3 TCR genes into NZB/W F_1 splenocytes induced a 40–45% increase in the $V\beta4^+$ population in $CD4^+$ T cells compared with mock-infected splenocytes (Fig. 1*B*). The calculated efficiency of the Vβ4 introduction into the

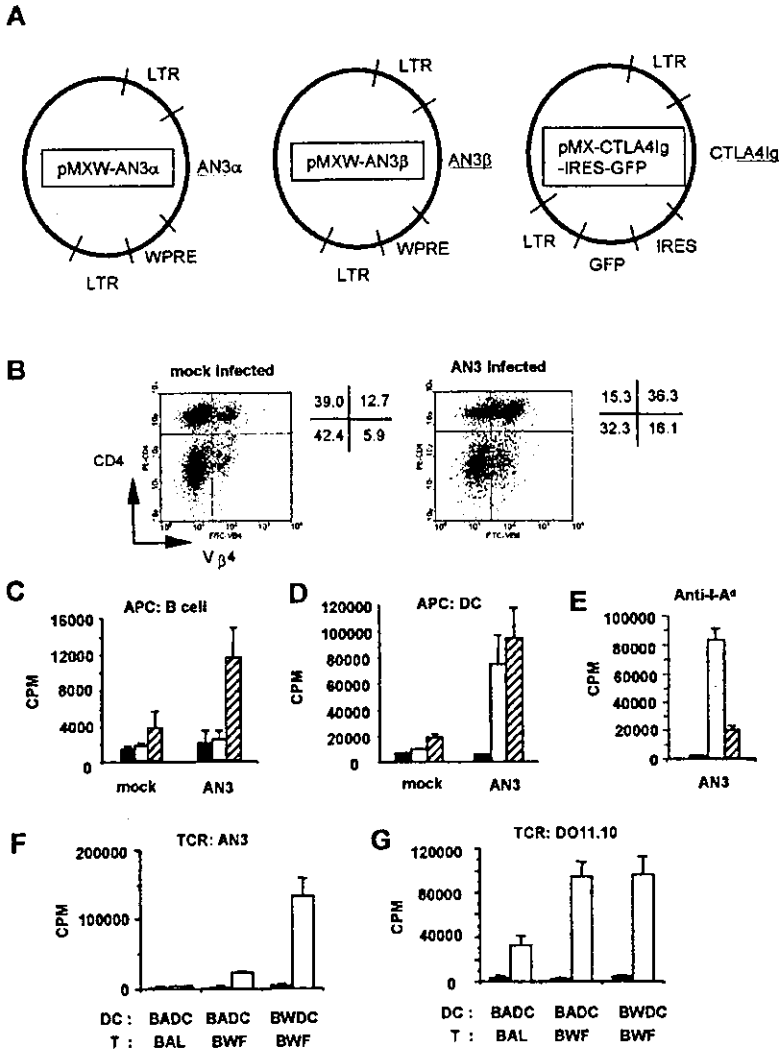

FIGURE 1. Retroviral transfer of AN3 TCR reconstituted the specificity for nucleosomes on NZB/W F_1 $CD4^+$ T cells. Reconstituted T cells showed autoreactivity to splenic DCs. *A*, Schematic representation of the pMXW retrovirus construct expressing the cDNA for the AN3 TCRα or TCRβ chain. LTR, long terminal repeat. *B*, Anti-CD4 and anti-Vβ4 staining of pMXW (mock) or AN3 TCR-transduced NZB/W F_1 splenocytes. Results of a representative experiment are shown. *C*, Proliferation of AN3-transduced and mock-transduced $CD4^+$ T cells to B cells with nucleosomes. ■, T cells alone; □, T + B; ▨, T + B + nucleosomes (1 μg/ml). *D*, Proliferation of AN3-transduced and mock-transduced $CD4^+$ T cells to $CD11c^+$ DCs with nucleosomes. ■, T cells alone; □, T + DCs; ▨, T + DCs + nucleosomes (1 μg/ml). *E*, Blockade of AN3-transduced $CD4^+$ T cell proliferation to NZB/W F_1 $CD11c^+$ DCs by an anti-I-A^d Ab, K24-199. ■, T cells alone; □, T + DCs; ▨, T + DCs + anti-I-A^d Ab. *F*, Proliferative response of AN3- or mock-transduced $CD4^+$ T cells from BALB/c (BAL) or NZB/W F_1 (BWF) (■, mock-transduced cells; □, AN3-transduced cells) with BALB/c $CD11c^+$ DCs (BADC) or NZB/W F_1 $CD11c^+$ DCs (BWDC). *G*, Proliferative response of DO11.10- and mock-transduced $CD4^+$ T cells from BALB/c (BAL) or NZB/W F_1 (BWF) (■, mock-transduced cells; □, DO11.10-transduced cells with 0.3 μM $OVA_{323-339}$) with BALB/c $CD11c^+$ DCs (BADC) or NZB/W F_1 $CD11c^+$ DCs (BWDC). Data shown are representative of more than three independent experiments with similar results.

$CD4^+V\beta4^-$ population was 50–60%. The lack of anti-Vα13 or anti-clonotypic Abs prevented direct visualization of AN3 TCR surface expression. However, based on the transduction of other TCR pairs (i.e., OVA-specific DO11.10 TCR detected by a clonotypic Ab KJ1-26; and AV8/BV7, detectable by anti-Vα8 and anti-Vβ7 Abs; data not shown), we speculate that Vα chain expression is approximately equal to that of the Vβ chain. Thus, the proportion of clonotypic AN3 TCR-expressing cells was estimated to be 25–36% in $CD4^+$ T cells. These cells were referred to as BWF.AN3, and the mock-infected $CD4^+$ T cells were referred to as BWF.mock.

We investigated the specific reactivity to the nucleosomes of BWF.AN3 in the presence of NZB/W F_1 B cells and DCs. Although BWF.mock cells showed minimal proliferation in the presence of B cells and the nucleosomes, BWF.AN3 showed strong proliferation in the presence of B cells and the nucleosomes, but not in the presence of B cells alone (Fig. 1*C*). The average ratio of (BWF.AN3 - cpm)/(BWF.mock − cpm) was 1.13 ± 0.12 and that of (BWF.AN3 with nucleosome (nuc) − cpm)/(BWF.mock with nuc − cpm) was 3.12 ± 0.51 in three experiments ($p < 0.005$). These results demonstrate that the introduction of AN3 TCR reconstitutes the specificity for the nucleosome on $CD4^+$ T cells. Furthermore, BWF.AN3 showed proliferation in the presence of splenic DCs without nucleosome (Fig. 1*D*). The average ratio of (BWF.AN3 − cpm)/(BWF.mock − cpm) was 6.97 ± 1.63 in five experiments ($p < 0.001$). Consistent with previous report that $CD4^+$ T cells of lupus-prone mice responded to nucleosome ex vivo (7), BWF.mock showed relatively weak proliferation in the presence of splenic DCs and nucleosome. The average ratio of (BWF.mock with nuc − cpm)/(BWF.mock − cpm) was 2.21 ± 0.73 in five experiments ($p < 0.05$). Despite these endogenous responses of BWF.mock to nucleosome, BWF.AN3 showed stronger proliferation compared with BWF.mock in the presence of splenic DCs with the nucleosomes. The average ratio of (BWF.AN3 with nuc − cpm)/(BWF.mock with nuc − cpm) was 4.01 ± 2.18 in five experiments ($p < 0.05$).

AN3α-infected or β-infected cells failed to respond to the DCs (data not shown), and the autoreactive response was blocked by anti-I-A^d Ab (Fig. 1*E*). Thus, this autoreactivity of BWF.AN3 to splenic DCs suggests that NZB/W F_1 splenic DCs spontaneously present a considerable amount of nucleosomal epitopes.

The nucleosome-specific response of NZB/W F_1 mice consisted of general T cell hyperreactivity and Ag-specific hyperpresentation of splenic DCs

To investigate the relative contribution of either T cells or splenic DCs to the autoreactive response, we also transduced the AN3 TCR into BALB/c $CD4^+$ T cells and these cells were referred to

as BAL.AN3. Although BAL.AN3 showed no proliferative response to BALB/c splenic DCs, BWF.AN3 showed a moderate proliferative response to BALB/c splenic DCs (Fig. 1*F*). These results suggest that the BWF1 T cell hyperreactivitiy enables BWF.AN3 to recognize small amounts of nucleosomal epitope presented on BALB/c splenic DCs, but these small amounts are ignored by BAL.AN3. As expected, BWF.AN3 strongly responded to BWF1 splenic DCs. Proliferative response of BWF.AN3 in the presence of BALB/c splenic DCs amounted to ~14–18% of that to BWF1 splenic DCs, indicating that the abnormal presentation of splenic DCs may contribute more to the autoreactive response than does T cell hyperreactivity.

To determine the general Ag recognition and reactivity of NZB/W F_1 mice, we examined the proliferation of T cells transduced with OVA-specific TCR (DO11.10). Fifty to 60% of the total $CD4^+$ T cells expressed the introduced DO11.10 TCR, as determined by the anti-clonotypic Ab KJ1-26. DO11.10-transduced BWF1 T cells cultured with DCs plus $OVA_{323-339}$ peptide exhibited stronger proliferation than BALB/c T cells, again suggesting that BWF1 T cells possess general hyperreactivity. In contrast, the OVA peptide-presentation (Fig. 1*G*) and the whole OVA presentation (data not shown) of NZB/W F_1 splenic DCs appeared to be quite similar to that of BALB/c splenic DCs. Thus, the hyperpresentation of DCs seems to be restricted to a certain Ag.

Nucleosome-specific T cells interacted with the autoantigen in the spleen

DCs in every type of lymphoid tissue may present nucleosomal epitopes, because nucleosomal Ags are available in every organ. To investigate this possibility, we fluorescently labeled either BWF.mock or BWF.AN3 T cells in vitro with CFSE and injected them into NZB/W F_1 mice. Two days after the transfer, T cells from the spleen and those from the peripheral lymph nodes (LNs) were harvested and analyzed. BWF.mock isolated from the spleen exhibited a convergent strong fluorescence peak, indicating that these cells had not proliferated extensively. In contrast, BWF.AN3 isolated from the spleen exhibited several weaker fluorescence peaks. Moreover, AN3 $CD4^+$ T cells underwent multiple divisions over a 5-day period of the experiment, and mock $CD4^+$ T cells underwent a very slight progression of cell division (Fig. 2*A*). These findings suggested that BWF.AN3 encountered the nucleosomal epitope in the spleen. It was of note that both CFSE-labeled BWF.mock and BWF.AN3 isolated from the peripheral LNs exhibited a strong convergent fluorescence peak, suggesting that BWF.AN3 encountered the nucleosomal epitope less frequently in the LNs.

A comparison of the stimulative capacity for BWF.AN3 also suggested that splenic DCs presented more nucleosomal epitope than DCs from the peripheral LNs (Fig. 2*B*). The average ratio of (BWsplDC − cpm)/(BWLNDC − cpm) was 2.79 ± 0.44 in three experiments ($p < 0.005$). These results showed that nucleosome-specific T cells are stimulated predominantly in the spleen.

Effect of CTLA4Ig transfer on the nucleosomal response

We next tried to generate nucleosome-specific regulatory cells by introducing an immunosuppressive molecule, CTLA4Ig, as the third gene in BWF.AN3 T cells. Long-term administration of CTLA4Ig to NZB/W F_1 mice has been shown to prevent disease onset for a period of months (29).

We constructed a pMX-CTLA4Ig-IRES-GFP vector (Fig. 1*A*). We then performed a triple gene transfer of the AN3$\alpha\beta$ and CTLA4Ig genes to investigate the effect on CTLA4Ig expression. The experimental groups consisted of $CD4^+$ T cells transduced with either AN3 + CTLA4Ig-IRES-GFP(CTLA4Ig), AN3 + IRES-GFP(IG), pMXW(mock) + CTLA4Ig, or mock + IG. The average expression efficiency from several different sets of infection was 45.2% for Vβ4 and 47.3% for GFP in $CD4^+$ cells (Fig. 3*A*). The average expression efficiency is expected to be 45% for the AN3α gene, and the average percentage of GFP^+AN3^+ cells expressing all three gene products in $CD4^+$ T cells was estimated to be ~10% (0.45 × 0.45 × 0.45). As shown in Fig. 3*B*, the CTLA4Ig secreted from T cells blocked the proliferation of the endogenous T cell population to the nucleosome to a moderate degree. The average ratio of (mock + CTLA4Ig with nuc − cpm)/(mock + IG with nuc − cpm) was 0.40 ± 0.07 in three experiments ($p < 0.005$). But the T cell stimulation mediated by AN3 TCR was not blocked by CTLA4Ig. The average ratio of (AN3 + IG − cpm)/(mock + IG − cpm) was 7.85 ± 1.07 and that of (AN3 + CTLA4Ig − cpm)/(mock + IG − cpm) was 7.18 ± 0.96 in three experiments. The AN3 + CTLA4Ig transduced cells showed the increase of CTLA4Ig secretion on T cell activation in the presence of DCs (Fig. 3*C*).

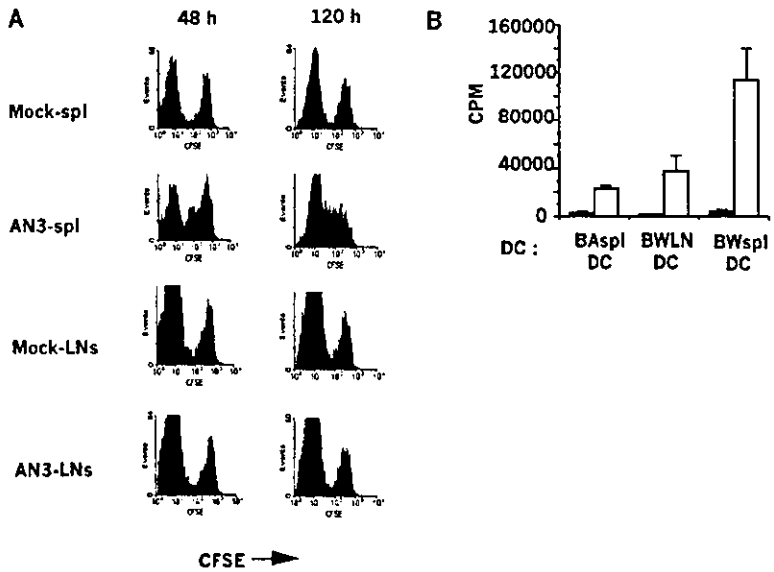

FIGURE 2. Nucleosome-specific T cells were stimulated more strongly in the spleen than in the LNs. *A*, CFSE-labeled BWF_1.mock T cells or BWF.AN3 T cells were transferred i.v. into 10-wk-old NZB/W F_1 mice. Two and 5 days later, splenocytes or peripheral LNs (cervical, inguinal, and mesenteric) from recipient mice were examined for $CFSE^+V\beta4^+$-gated cells. *B*, Proliferation of AN3- or mock-transduced T cells to $CD11c^+$ DCs from the spleen or LNs. $CD11c^+$ DCs from NZB/W F_1 spleens (BWsplDC), from NZB/W F_1 LNs (BWLNDC) and from BALB/c spleens (BAsplDC). Data shown are representative of three independent experiments with similar results.

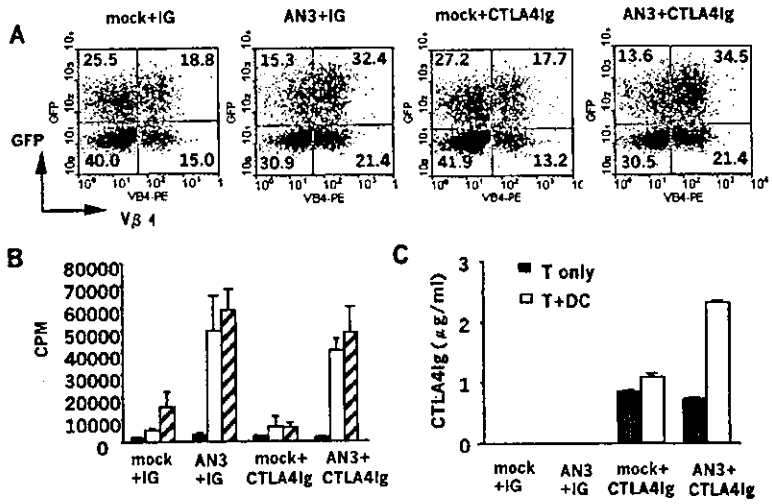

FIGURE 3. Effect of CTLA4Ig gene transfer on the T cell proliferation to nucleosomes. *A,* Expression analysis of GFP and Vβ4 in gene-transduced cells gated for CD4. The transduction efficiency was ~45% for a single gene in each group. *B,* Suppressive effect of CTLA4Ig transduction on T cell activation to nucleosomes. ■, T cells alone; □, T + DCs; ▨, T + DCs + nucleosome. *C,* CTLA4Ig production of T cells with or without DCs. Each culture supernatant was harvested after 24 h of culture. Data shown are representative of three independent experiments with similar results.

Nucleosome-specific regulatory cells suppressed autoimmune disease

We transferred cell suspensions containing 1×10^6 cells of $CD4^+$ T cells, calculatedly expressing either AN3 + CTLA4Ig, AN3 + IG, mock + CTLA4Ig, or mock + IG into 10-wk-old NZB/W F_1 mice.

The autoantibodies usually found in NZB/W F_1 mice were measured in the sera from the different groups. The elevations of anti-dsDNA and anti-histone Abs were suppressed in AN3 + CTLA4Ig-injected mice at 22 wk of age (Fig. 4*A*). AN3 + CTLA4Ig-injected mice showed the lowest average titer of anti-nucleosome Ab, but the titer in this group was not significantly different from those in the controls. This inefficient suppression may be due to the fact that autoimmunity to the nucleosome is the driving reaction and that this reaction is stronger than the subsequent response.

The mice were monitored biweekly for proteinuria. By week 22, control mice that had received PBS, mock + IG, AN3 + IG, or

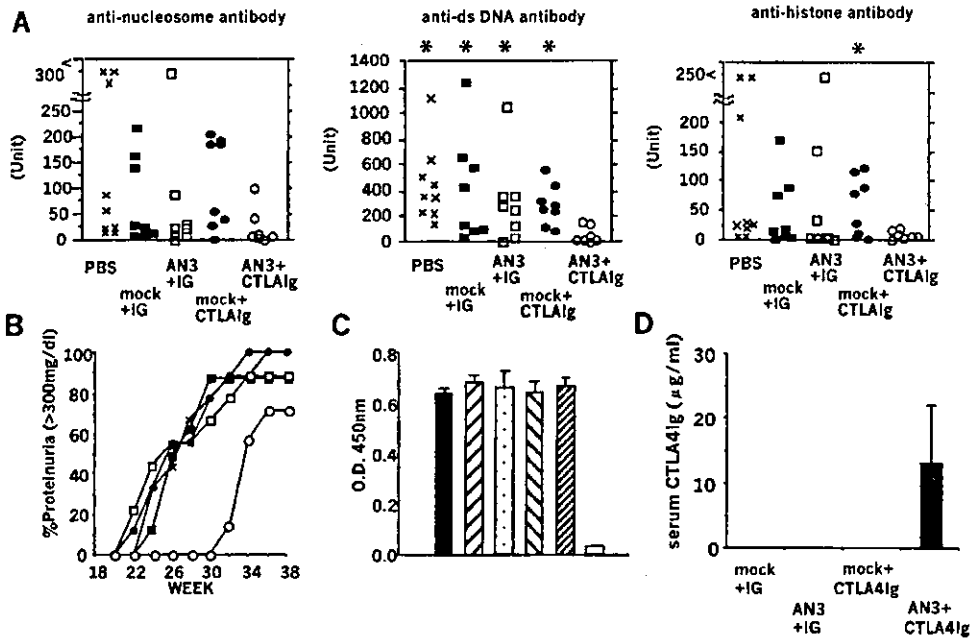

FIGURE 4. Effect of adoptively transferred engineered cells on disease progression. *A,* Suppression of autoantibody production. The elevation of serum anti-nucleosome, anti-dsDNA, and anti-histone Abs, measured by ELISA, was suppressed in AN3 + CTLA4Ig-injected mice at 22 wk. Statistically significant differences between AN3 + CTLA4Ig and control groups are denoted by asterisks ($p < 0.05$); $n = 7$ for AN3 + CTLA4Ig, and $n = 8$ for each control group. *B,* Cumulative percentage of mice in each group that developed severe proteinuria (>300 mg/dl). AN3 + CTLA4Ig showed suppressed progression of proteinuria compared with the control groups. x, PBS; ■, mock + IG; □, AN3 + IG; ●, mock + CTLA4Ig; ○, AN3 + CTLA4Ig. AN3 + CTLA4Ig vs the controls at 30 wk was significant ($p < 0.05$). *C,* A T cell-dependent humoral immune response to active immunization of OVA. Mice transferred with the engineered T cells at 10 wk of age were immunized with OVA in the footpad at 14 wk of age. Anti-OVA IgG Ab titer was measured at 17 wk of age. ■, PBS; ▨, mock + IG; ▨, AN3 + IG; ▨, mock + CTLA4Ig; ▨, AN3 + CTLA4Ig; □, no immunization. $n = 6$/group. *D,* Measurement of serum CTLA4Ig protein in the experimental groups with ELISA. Only AN3 + CTLA4Ig-transferred mice showed detectable, but low concentration of CTLA4Ig protein.

mock + CTLA4Ig started developing severe nephritis, as diagnosed by persistent proteinuria of >300 mg/dl. By 30 wk of age, 89% of the PBS control group, 88% of the mock + IG group, 63% of the AN3 + IG group, and 75% of the mock + CTLA4Ig group of mice had developed severe proteinuria, whereas none of the AN3 + CTLA4Ig mice showed excess proteinuria (Fig. 4*B*). However, the AN3 + CTLA4Ig-transferred mice started to develop severe proteinuria at 32 wk of age. Splenomegaly and an increase in the CD4:CD8 ratio, usually observed in aged NZB/W F_1 mice, were suppressed in AN3 + CTLA4Ig-injected mice (data not shown).

The kidneys from the controls and AN3 + CTLA4Ig-injected mice were examined at 30 wk of age (Fig. 5, *A–F*). Control mice had severe glomerulonephritis with mesangial proliferation and thickening of the capillary walls with marked deposition of IgG and complement. AN3 + CTLA4Ig-injected mice had mild glomerular lesions and deposition of IgG and complement was only restricted to the mesangial area. Although mock + CTLA4Ig-transferred mice showed formation of a number of large follicles with T cell invasion in the spleen, AN3 + CTLA4Ig-transferred mice showed only a limited number of small follicles (Fig. 5, *G* and *H*).

AN3 + CTLA4Ig-treated mice exhibited the normal humoral immune response upon active immunization

We next examined the T cell-dependent humoral immune response to active immunization of OVA. Mice transferred with the engineered T cells at 10 wk of age were immunized with OVA (100 μg) with CFA at 14 wk of age and boosted with OVA with IFA at 16 wk of age. The level of anti-OVA IgG Ab titer from 17-wk-old mice treated with AN3 + CTLA4Ig was not significantly different from those of the control mice (Fig. 4*C*). AN3 + CTLA4Ig transferred mice, but not other experimental groups, had low but detectable levels of serum CTLA4Ig (13.4 ± 10.1 μg/ml) (Fig. 4*D*), findings consistent with in vitro data shown in Fig. 3*C*. These results suggest that the engineered regulatory cells are sufficient to suppress autoimmune disease. However, they are not enough to induce general immunosuppression, because of the low serum level of CTLA4Ig in AN3 + CTLA4Ig-transferred mice.

Discussion

In this study, we demonstrated T cell hyperresponsiveness and the possibility of nucleosomal hyperpresentation of splenic DCs in NZB/W F_1 mice. In addition to the involvement of T cell hyperresponsiveness in Ab-mediated autoimmune disease (30), our results strongly suggest that the autoantigen hyperpresentation of DCs could contribute to the initiation and propagation of the response to the autoantigen, thereby resulting in florid autoimmune disease. This observation is consistent with those from previous reports indicating that mice with T cell hyperresponsiveness develop only a mild form of lupus-like symptoms (31, 32). Since hyperpresentation was not observed in the case of an exogenous Ag, OVA (peptides and whole protein), it is possible that the autoantigen hyperpresentation of splenic DCs was not due to the general hyperpresentation, e.g., excessive costimulatory signals, but rather to some Ag-restricted phenomenon. These features may be nucleosome specific, as reported in a previous study demonstrating that lupus-prone B6.NZMc1 mice showed nucleosome reactivity of T cells without generalized immunological deficits of B cells and T cells (33).

Although disease-related increases in the number of splenic DCs and chemokine production by myeloid DCs have been reported (34), these abnormalities have been observed in aged lupus-prone mice. Our finding of autoantigen hyperpresentation in the splenic DCs of young mice (10 wk) suggests the significance of the autoantigen hyperpresentation of splenic DCs in the pathogenesis of lupus.

Autoreactive response of nucleosome-specific T cells was much more prominent in the spleen than in the LNs. Although the mixed I-A haplotype of Aβz/Aαd molecules in NZB/W F_1 mice (35) may be associated with autoreactive response of AN3 infectant, the absence of the autoreactivity to B cells and DCs from peripheral LNs strongly suggests the requirement of an autoantigen for the autoreactivity. Differences between the splenic DCs and DCs from other peripheral lymphoid organs have been reported, including differences in the expression of chemokines (36) and chemokine receptors (37). Otherwise, localization of tissue-specific autoantigen among secondary lymphoid organs may be one explanation. For example, although DCs in the gastric LNs are known to exhibit constitutive presentation of gastric parietal cell-specific H^+/K^+-ATPase, peripheral or mesenteric DCs do not (38). Thus, the spleen could be one of the main sources of nucleosomes. Increased frequency of splenic apoptosis in SNF1 lupus mice has also been reported (23). Moreover, an insufficient complement system may allow apoptotic waste material to accumulate in the spleen (i.e., the "waste disposal" hypothesis) (39).

In our study, the therapeutic effect with minimal systemic immunosuppression was archived by the use of nucleosome-specific T cells secreting CTLA4Ig. Although elevation of CTLA4Ig protein was detected in the serum of AN3 + CTLA4Ig mice, the

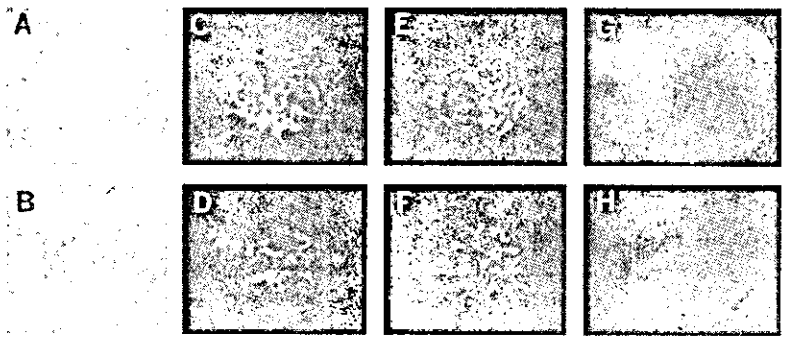

FIGURE 5. Histological examination from the AN3 + CTLA4Ig-treated mice compared with control mice. Sections of kidney from mock + IG-injected mice (*A*, *C*, and *E*) and AN3 + CTLA4Ig-injected mice (*B*, *D*, and *F*) subjected to staining with periodic-acid-Schiff solution (*A* and *B*) or to immunofluorescence staining with anti-IgG (*C* and *D*) or anti-C3 (*E* and *F*). Immunofluorescence staining of sections from the spleen, from mock + CTLA4Ig-injected mice (*G*), and from AN3 + CTLA4Ig-injected mice (*H*) with Abs to B220 (green), CD4 and CD8 (red), and with peanut agglutinin (blue). A section from one representative mouse from the indicated group is shown.

average concentration of CTLA4Ig in AN3 + CTLA4Ig mice is less than one-tenth of the level of previous systemic CTLA4Ig treatment with 5×10^8 PFU of adenovirus (27). Although the systemic adenoviral-CTLA4Ig (5×10^8 PFU) treatment exhibited a therapeutic effect equivalent to that of our experiment, the systemic treatment was accompanied with generalized immunosuppression. Since autoantigen-specific CTLA4Ig-secreting T cells showed normal Ab production on active immunization, this treatment may be superior to systemic CTLA4Ig administration. However, a systemic effect of a very low level of CTLA4Ig cannot be excluded and should be investigated further.

It is not surprising that 10^6 AN3 + mock cells did not aggravate the disease, since as many as 4×10^7 original L3A clone cells were needed to accelerate lupus nephritis in young lupus-prone mice (40). Thus, a relatively small amount of Ag-specific and potentially pathogenic T cells could be used for the immunotherapy. Foxp3, a member of the transcription factor family, has been identified as a key molecule for the development of $CD4^+CD25^+$ regulatory T cells (41). Retroviral transfer of Foxp3 confers regulatory function on $CD4^+CD25^-$ T cells. The introduction of such regulatory molecules with TCR could possibly generate Ag-specific regulatory T cells.

In a preliminary analysis of the persistence of the transferred genes in the spleen and LNs from 30-wk-old mice with RT-PCR, expression of AN3α gene was detected in the spleens from two of two AN3 + IG^- and AN3 + CTLA4Ig^--injected mice (data not shown). These results may suggest the persistence of introduced genes at 20 wk after the transfer in the spleen.

Although several models of adoptive cell gene therapy have been reported using T cell hybridomas or lines (42, 43), our method has the advantage of using autologous lymphocytes for gene recipients. However, TCR-transduced recipient T cells could gain heterodimeric TCR consisting of endogenous and exogenous chains. If such an unexpected TCR recognizes a certain unrelated self-derived molecule, the transduced T cells may be harmful. We did not observe evident autoreactivity in single AN3α or AN3β genes transferred into $CD4^+$ T cells (data not shown), and the renal disease of AN3 TCR-transferred mice was not accelerated (Fig. 5*B*). There was a recent report of tumor rejection mediated by retrovirally reconstituted Ag-specific T cells without any significant autoimmune pathology (44, 45). However, the possibility of developing autoimmunity should be carefully investigated further in application of TCR gene transfer.

In the present study, the efficacy of triple gene transfer in peripheral T cells was demonstrated for the first time. Although several improvements of the present method are still necessary, these findings suggest that the direct engineering of Ag-specific functional cells with multiple gene transfer is a powerful technique for the development of future Ag-specific therapies.

Acknowledgments

We are grateful to Kazumi Abe and Shiho Ohta for their excellent technical assistance.

References

1. Zitvogel, L., J. I. Mayordomo, T. Tjandrawan, A. B. DeLeo, M. R. Clarke, M. T. Lotze, and W. J. Storkus. 1996. Therapy of murine tumors with tumor peptide-pulsed dendritic cells: dependence on T cells, B7 costimulation, and T helper cell 1-associated cytokines. *J. Exp. Med. 183:87.*
2. Nestle, F. O., S. Alijagic, M. Gilliet, Y. Sun, S. Grabbe, R. Dummer, G. Burg, and D. Schadendorf. 1998. Vaccination of melanoma patients with peptide- or tumor lysate-pulsed dendritic cells. *Nat. Med. 4:328.*
3. Steinberg, A. D., M. F. Gourley, D. M. Klinman, G. C. Tsokos, D. E. Scott, and A. M. Krieg. 1991. NIH conference: systemic lupus erythematosus. *Ann. Intern. Med. 115:548.*
4. Lambert, P. H., and F. J. Dixon. 1968. Pathogenesis of the glomerulonephritis of NZB/W mice. *J. Exp. Med. 127:507.*
5. Dixon, F. J., M. B. Oldstone, and G. Tonietti. 1971. Pathogenesis of immune complex glomerulonephritis of New Zealand mice. *J. Exp. Med. 134(Suppl.):65s.*
6. Winfield, J. B., I. Faiferman, and D. Koffler. 1977. Avidity of anti-DNA antibodies in serum and IgG glomerular eluates from patients with systemic lupus erythematosus: association of high avidity antinative DNA antibody with glomerulonephritis. *J. Clin. Invest. 59:90.*
7. Mohan, C., S. Adams, V. Stanik, and S. K. Datta. 1993. Nucleosome: a major immunogen for pathogenic autoantibody-inducing T cells of lupus. *J. Exp. Med. 177:1367.*
8. Kaliyaperumal, A., C. Mohan, W. Wu, and S. K. Datta. 1996. Nucleosomal peptide epitopes for nephritis-inducing T helper cells of murine lupus. *J. Exp. Med. 183:2459.*
9. Lu, L., A. Kaliyaperumal, D. T. Boumpas, and S. K. Datta. 1999. Major peptide autoepitopes for nucleosome-specific T cells of human lupus. *J. Clin. Invest. 104:345.*
10. Burlingame, R. W., R. L. Rubin, R. S. Balderas, and A. N. Theofilopoulos. 1993. Genesis and evolution of antichromatin autoantibodies in murine lupus implicates T-dependent immunization with self antigen. *J. Clin. Invest. 91:1687.*
11. Burlingame, R. W., M. L. Boey, G. Starkebaum, and R. L. Rubin. 1994. The central role of chromatin in autoimmune responses to histones and DNA in systemic lupus erythematosus. *J. Clin. Invest. 94:184.*
12. Amoura, Z., S. Koutouzov, H. Chabre, P. Cacoub, I. Amoura, L. Musset, J. F. Bach, and J. C. Piette. 2000. Presence of antinucleosome autoantibodies in a restricted set of connective tissue diseases: antinucleosome antibodies of the IgG3 subclass are markers of renal pathogenicity in systemic lupus erythematosus. *Arthritis Rheum. 43:76.*
13. Bruns, A., S. Blass, G. Hausdorf, G. R. Burmester, and F. Hiepe. 2000. Nucleosomes are major T and B cell autoantigens in systemic lupus erythematosus. *Arthritis Rheum. 43:2307.*
14. Desai-Mehta, A., L. Lu, R. Ramsey-Goldman, and S. K. Datta. 1996. Hyperexpression of CD40 ligand by B and T cells in human lupus and its role in pathogenic autoantibody production. *J. Clin. Invest. 97:2063.*
15. Liossis, S. N., B. Kovacs, G. Dennis, G. M. Kammer, and G. C. Tsokos. 1996. B cells from patients with systemic lupus erythematosus display abnormal antigen receptor-mediated early signal transduction events. *J. Clin. Invest. 98:2549.*
16. Wofsy, D., and W. E. Seaman. 1985. Successful treatment of autoimmunity in NZB/NZW F_1 mice with monoclonal antibody to L3T4. *J. Exp. Med. 161:378.*
17. Donello, J. E., J. E. Loeb, and T. J. Hope. 1998. Woodchuck hepatitis virus contains a tripartite posttranscriptional regulatory element. *J. Virol. 72:5085.*
18. Zufferey, R., J. E. Donello, D. Trono, and T. J. Hope. 1999. Woodchuck hepatitis virus posttranscriptional regulatory element enhances expression of transgenes delivered by retroviral vectors. *J. Virol. 73:2886.*
19. Kitamura, T., M. Onishi, S. Kinoshita, A. Shibuya, A. Miyajima, and G. P. Nolan. 1995. Efficient screening of retroviral cDNA expression libraries. *Proc. Natl. Acad. Sci. USA 92:9146.*
20. Wallace, P. M., J. S. Johnson, J. F. MacMaster, K. A. Kennedy, P. Gladstone, and P. S. Linsley. 1994. CTLA4Ig treatment ameliorates the lethality of murine graft-versus-host disease across major histocompatibility complex barriers. *Transplantation 58:602.*
21. Kawashima, T., K. Hirose, T. Satoh, A. Kaneko, Y. Ikeda, Y. Kajiro, T. Nosaka, and T. Kitamura. 2000. MgcRacGAP is involved in the control of growth and differentiation of hematopoietic cells. *Blood 96:2116.*
22. Fujio, K., Y. Misaki, K. Setoguchi, S. Morita, K. Kawahata, I. Kato, T. Nosaka, K. Yamamoto, and T. Kitamura. 2000. Functional reconstitution of class II MHC-restricted T cell immunity mediated by retroviral transfer of the $\alpha\beta$ TCR complex. *J. Immunol. 165:528.*
23. Morita, S., T. Kojima, and T. Kitamura. 2000. Plat-E: an efficient and stable system for transient packaging of retroviruses. *Gene Ther. 7:1063.*
24. Kalled, S. L., A. H. Cutler, and L. C. Burkly. 2001. Apoptosis and altered dendritic cell homeostasis in lupus nephritis are limited by anti-CD154 treatment. *J. Immunol. 167:1740.*
25. Akbari, O., R. H. DeKruyff, and D. T. Umetsu. 2001. Pulmonary dendritic cells producing IL-10 mediate tolerance induced by respiratory exposure to antigen. *Nat. Immunol. 2:725.*
26. Bates, D. L., P. J. Butler, E. C. Pearson, and J. O. Thomas. 1981. Stability of the higher-order structure of chicken-erythrocyte chromatin in solution. *Eur. J. Biochem.119:469*
27. Mihara, M., I. Tan, Y. Chuzhin, B. Reddy, L. Budhai, A. Holzer, Y. Gu, and A. Davidson. 2000. CTLA4Ig inhibits T cell-dependent B-cell maturation in murine systemic lupus erythematosus. *J. Clin. Invest. 106:91.*
28. Shi, Y., A. Kaliyaperumal, L. Lu, S. Southwood, A. Sette, M. A. Michaels, and S. K. Datta. 1998. Promiscuous presentation and recognition of nucleosomal autoepitopes in lupus: role of autoimmune T cell receptor α chain. *J. Exp. Med. 187:367.*
29. Finck, B. K., P. S. Linsley, and D. Wofsy. 1994. Treatment of murine lupus with CTLA4Ig. *Science 265:1225.*
30. Vratsanos, G. S., S. Jung, Y. M. Park, and J. Craft. 2001. $CD4^+$ T cells from lupus-prone mice are hyperresponsive to T cell receptor engagement with low and high affinity peptide antigens: a model to explain spontaneous T cell activation in lupus. *J. Exp. Med. 193:329.*
31. Murga, M., O. Fernandez-Capetillo, S. J. Field, B. Moreno, L. R. Borlado, Y. Fujiwara, D. Balomenos, A. Vicario, A. C. Carrera, S. H. Orkin, M. E. Greenberg, and A. M. Zubiaga. 2001. Mutation of E2F2 in mice causes enhanced T lymphocyte proliferation, leading to the development of autoimmunity. *Immunity 15:959.*

32. Mohan, C., Y. Yu, L. Morel, P. Yang, and E. K. Wakeland. 1999. Genetic dissection of Sle pathogenesis: Sle3 on murine chromosome 7 impacts T cell activation, differentiation, and cell death. *J. Immunol. 162:6492.*
33. Mohan, C., E. Alas, L. Morel, P. Yang, and E. K. Wakeland. 1998. Genetic dissection of SLE pathogenesis: Sle1 on murine chromosome 1 leads to a selective loss of tolerance to H2A/H2B/DNA subnucleosomes. *J. Clin. Invest. 101: 1362.*
34. Ishikawa, S., T. Sato, M. Abe, S. Nagai, N. Onai, H. Yoneyama, Y. Zhang, T. Suzuki, S. Hashimoto, T. Shirai, M. Lipp, and K. Matsushima. 2001. Aberrant high expression of B lymphocyte chemokine (BLC/CXCL13) by $C11b^+CD11c^+$ dendritic cells in murine lupus and preferential chemotaxis of B1 cells towards BLC. *J. Exp. Med. 193:1393.*
35. Gotoh, Y., H. Takashima, K. Noguchi, H. Nishimura, M. Tokushima, T. Shirai, and M. Kimoto. 1993. Mixed haplotype Abz/Aad class II molecule in (NZB × NZW)F_1 mice detected by T cell clones. *J. Immunol. 150: 4777.*
36. Yoneyama, H., S. Narumi, Y. Zhang, M. Murai, M. Baggiolini, A. Lanzavecchia, T. Ichida, H. Asakura, and K. Matsushima. 2002. Pivotal role of dendritic cell-derived CXCL10 in the retention of T helper cell 1 lymphocytes in secondary lymph nodes. *J. Exp. Med. 195:1257.*
37. Iwasaki, A., and B. L. Kelsall. 2000. Localization of distinct Peyer's patch dendritic cell subsets and their recruitment by chemokines macrophage inflammatory protein (MIP)-3α, MIP-3β, and secondary lymphoid organ chemokine. *J. Exp. Med. 191:1381.*
38. Scheinecker, C., R. McHugh, E. M. Shevach, and R. N. Germain. 2002. Constitutive presentation of a natural tissue autoantigen exclusively by dendritic cells in the draining lymph node. *J. Exp. Med. 196:1079.*
39. Walport, M. J. 2001. Complement. *N. Engl. J. Med. 344:1140.*
40. Adams, S., P. Leblanc, and S. K. Datta. 1991. Junctional region sequences of T-cell receptor β-chain genes expressed by pathogenic anti-DNA autoantibody-inducing helper T cells from lupus mice: possible selection by cationic autoantigens. *Proc. Natl. Acad. Sci. USA 88:11271.*
41. Hori, S., T. Nomura, and S. Sakaguchi. 2003. Control of regulatory T cell development by the transcription factor Foxp3. *Science 299:1057.*
42. Setoguchi, K., Y. Misaki, Y. Araki, K. Fujio, K. Kawahata, T. Kitamura, and K. Yamamoto. 2000. Antigen-specific T cells transduced with IL-10 ameliorate experimentally induced arthritis without impairing the systemic immune response to the antigen. *J. Immunol. 165:5980.*
43. Nakajima, A., C. M. Seroogy, M. R. Sandora, I. H. Tamer, G. L. Costa, C. Taylor-Edwards, M. H. Bachmann, C. H. Contag, and C. G. Fathman. 2001. Antigen-specific T cell-mediated gene therapy in collagen-induced arthritis. *J. Clin. Invest. 107:1293.*
44. Kessels, H. W., M. C. Wolkers, M. D. van den Boom, M. A. van der Valk, and T. N. Schumacher. 2001. Immunotherapy through TCR gene transfer. *Nat. Immunol. 2:957.*
45. Schumacher, T. N. 2002. T-cell-receptor gene therapy. *Nat. Rev. Immunol. 2:512.*

Dissection of the role of MHC class II A and E genes in autoimmune susceptibility in murine lupus models with intragenic recombination

Danqing Zhang*, Keishi Fujio†, Yi Jiang‡, Jingyuan Zhao*, Norihiro Tada§, Katsuko Sudo¶, Hiromichi Tsurui*, Kazuhiro Nakamura*, Kazuhiko Yamamoto†, Hiroyuki Nishimura‖, Toshikazu Shirai*, and Sachiko Hirose*,**

*Second Department of Pathology and §Atopy Research Center, Juntendo University School of Medicine, Tokyo 113-8421, Japan; †Department of Allergy and Rheumatology, Graduate School of Medicine, University of Tokyo, Tokyo 113-0033, Japan; ‡Central Laboratory of First Clinical College, China Medical University, ShenyCang 110001, China; ¶Animal Research Center, Tokyo Medical University, Tokyo 160-8402, Japan; and ‖Toin Human Science and Technology Center, Department of Biomedical Engineering, Toin University of Yokohama, Yokohama 225-8502, Japan

Communicated by N. Avrion Mitchison, University College London, London, United Kingdom, August 8, 2004 (received for review July 7, 2004)

Systemic lupus erythematosus (SLE) is a multigenic autoimmune disease, and the major histocompatibility complex (MHC) class II polymorphism serves as a key genetic element. In SLE-prone (NZB × NZW)F_1 mice, the MHC H-$2^{d/z}$ heterozygosity (H-2^d of NZB and H-2^z of NZW) has a strong impact on disease; thus, congenic H-$2^{d/d}$ homozygous F_1 mice do not develop severe disease. In this study, we used *Ea*-deficient intra-H-2 recombination to establish $A^{d/d}$-congenic (NZB × NZW)F_1 mice, with or without E molecule expression, and dissected the role of class II A and E molecules. Here we found that $A^{d/d}$ homozygous F_1 mice lacking E molecules developed severe SLE similar to that seen in wild-type F1 mice, including lupus nephritis, autoantibody production, and spontaneously occurring T cell activation. Additional evidence revealed that E molecules prevent the disease in a dose-dependent manner; however, the effect is greatly influenced by the haplotype of A molecules, because wild-type H-$2^{d/z}$ F_1 mice develop SLE, despite E molecule expression. Studies on the potential of dendritic cells to present a self-antigen chromatin indicated that dendritic cells from wild-type F_1 mice induced a greater response of chromatin-specific T cells than did those from $A^{d/d}$ F_1 mice, irrespective of the presence or absence of E molecules, suggesting that the self-antigen presentation is mediated by A, but not by E, molecules. Our mouse models are useful for analyzing the molecular mechanisms by which MHC class II regions regulate the process of autoimmune responses.

Systemic lupus erythematosus (SLE) is a systemic autoimmune disease characterized by the appearance of autoantibodies to several nuclear components. The deposition of formed immune complexes mediates the disease in a wide variety of tissues and organs, including the kidney and the vascular system. There is evidence that the development of SLE is under the control of multiple susceptibility genes (1). Among these, genes in the major histocompatibility complex (MHC) have been implicated as a key genetic element. Because SLE is an autoantibody-mediated disease, MHC class II polymorphisms are probably involved in the pathogenesis. However, because of the complex multifactorial inheritance and heterogeneity of SLE, and because of the linkage disequilibrium that exists among the class I, II, and III genes within the MHC complex, the absolute contribution of individual MHC class II loci has been difficult to dissect. Thus, our knowledge of the molecular mechanism of MHC class II contribution to SLE remains incomplete.

Substantial progress in research in this area has been achieved through studies using SLE-prone mice with genetic recombination and manipulation of MHC (H-2) genes. In (NZB × NZW)F_1 mice that spontaneously develop disease closely resembling human SLE, the disease is strongly associated with H-2 haplotypes from both parents (H-2^d from NZB and H-2^z from NZW) (2–6). Genetic dissection by producing H-2-congenic mice revealed that an early onset of severe SLE occurs in only heterozygous H-$2^{d/z}$ mice and not in homozygous H-$2^{d/d}$ and H-$2^{z/z}$ mice (2, 3, 5). Although both A and E class II molecules may be involved, evidence has suggested that mixed haplotype class II $A\alpha^d\beta^z$ molecules are responsible for the pathogenesis by promoting the production of pathogenic high-affinity IgG autoantibodies to nuclear components (7, 8).

In contrast to class II A molecules, E molecules are suggested to be a suppressive genetic element for SLE. This notion was based mainly on the results obtained by using a transgene technique. A BXSB strain of mouse, another spontaneous SLE model, carries H-2^b haplotype and expresses A^b, but not E, molecules, because of a defect in the *Ea* gene (9). The development of BXSB disease is closely associated with the H-2^b haplotype (10) and is almost completely prevented by a transgene encoding $E\alpha^d$ chains (11). Similar findings were noted in the nonobese diabetic (NOD) mouse, a model of spontaneous autoimmune diabetes. NOD mice express class II A^{g7}, but not E, molecules, because of a defect in the *Ea* gene (12). Evidence indicated that whereas the class II A^{g7} gene is critical for the disease susceptibility (13), the transgenic introduction of $E\alpha^d$ or $E\alpha^k$ does prevent the disease (14–16). Thus, A and E molecules seem to provide the susceptible and protective genetic elements for autoimmune diseases, respectively, at least in these mouse models.

Nevertheless, the conclusion awaits further studies, because the transgene possibly induces unexpected improper effects on immune cells. For example, unpaired or mispaired transgene-derived class II molecules can be toxic to B cell maturation (17). Furthermore, there are reports suggesting that excessively generated transgenic $E\alpha^d$ molecules bind to A molecules, thereby decreasing the availability of A molecules for antigen presentation (18), and that overexpression of E molecules suppresses expression levels of endogenously encoded A molecules (19). In the (NZB × NZW)F_1 model, severe SLE occurs despite the presence of intact E molecules. To examine the role of A and E molecules in (NZB × NZW)F_1 lupus, we generated several kinds of congenic (NZB × NZW)F_1 mice with intra-MHC recombination at the *E* subregion, taking advantage of natural recombinants, including those we found among ≈3,000 meiosis in crosses of NZB strains.

Materials and Methods

Mice. NZB (H-2^d) and NZW (H-2^z) mice were purchased from the Shizuoka Laboratory Animal Center (Shizuoka, Japan) and were maintained in our animal facility. The H-2-congenic

Abbreviations: DC, dendritic cell; NOD, nonobese diabetic; SLE, systemic lupus erythematosus; TCR, T cell receptor.

**To whom correspondence should be addressed at: Second Department of Pathology, Juntendo University School of Medicine, 2-1-1, Hongo, Bunkyo-ku, Tokyo 113-8421, Japan. E-mail: sacchi@med.juntendo.ac.jp.

www.pnas.org/cgi/doi/10.1073/pnas.0405807101

Table 1. H-2 haplotypes of established MHC-congenic and intra-MHC recombinant-congenic New Zealand strains of mice

Strains	H-2 haplotype	*K*	*Ab*	*Aa*	*Eb*		*Ea*		*Tnfa*	*D*
NZB	d	d	d	d	d		d		d	d
NZB.GD	g2	d	d	d	d	//	b		b	b
NZW.GD	g2	d	d	d	d	//	b		b	b
NZB.GDr	g2r	d	d	d	d		d	//	b	b
NZW.H-2^d	d	d	d	d	d		d		d	d
(NZB × NZW.H-2^d)F_1	d/d	d	d	d	d		d		d	d
(NZB × NZW.GD)F_1	d/g2	d	d	d	d		d/b		d/b	d/b
(NZB.GDr × NZW.GD)F_1	g2r/g2	d	d	d	d		d/b		b	b
(NZB.GD × NZW.GD)F_1	g2/g2	d	d	d	d	//	b		b	b

//, Intra-H-2 recombination site between d and b haplotype.

NZW.H-2^d (2, 3, 5) strain was established by selective backcrossing of (NZB × NZW)F_1 to NZW for 15 generations. NZB.GD (H-2^{g2}) (20) and NZW.GD strains were established by selective backcrossing of (B10.GD × NZB)F_1 and (B10.GD × NZW)F_1 with NZB and with NZW mice, respectively, for 15 generations. The NZB strain with an intragenic recombination between *Ea* of NZB and *Tnfa* of NZB.GD was obtained in crosses of NZB and NZB.GD strains and was tentatively designated NZB.GDr. Alleles at the H-2 loci in established H-2-congenic and recombinant H-2-congenic New Zealand mice are shown in Table 1. These mice were crossed to produce (NZB × NZW)F_1 hybrids with the same d haplotype of the upstream region of the *Eb* gene but with different haplotypes of downstream regions of the *Ea* gene (Table 1), and the disease severity was compared among these female F_1 mice.

Typing of H-2 Haplotype. Peripheral blood was obtained from the periorbital sinus, followed by lysis of red blood cells with ammonium chloride. Aliquots of 5×10^5 to 10×10^5 cells were incubated with anti-A^d (K24–199) (21); anti-E (ISCR, which reacts with a common determinant of the E molecule) (a kind gift from Dr. N. Shinohara, Kitasato University, Kanagawa, Japan); anti-D^d (T19–191); and anti-D^b (H141–30) mAbs, followed by FITC-labeled anti-mouse polyclonal IgG antibodies (ICN). Incubations were run for 30 min at 4°C, and the stained cells were analyzed by using FACSTAR and CELLQUEST software (Becton Dickinson).

Microsatellite DNA Polymorphism in the *Tnfa* Promoter. *Tnfa* promoter was shown to have microsatellite polymorphism, and different tumor necrosis factor alleles have different lengths of microsatellites (22, 23). To determine the tumor necrosis factor alleles of each mouse strain, PCRs were performed with genomic DNAs, using 5′ primer (5′-GGACAGAGAAGAAATGGGTTTC-3′) and 3′ primer (5′-TCGAATCTGGGGCCAATCAGGAGGG-3′) (22), and differences in lengths of PCR products were determined by using electrophoresis of PCR products on 7% denaturing polyacrylamide gels, as described in ref. 24.

Measurement of Proteinuria. The onset of renal disease was monitored by biweekly testing for proteinuria, as described in ref. 25. Mice with a proteinuria of 111 mg/ml or more in repeated tests were regarded as being positive.

Measurements of Anti-DNA and Anti-Chromatin Antibodies. Serum levels of IgG autoantibodies to DNA and chromatin were determined by ELISA, using peroxidase-conjugated polyclonal anti-mouse IgG antibodies (ICN). The DNA- and chromatin-binding activities were expressed in units, referring to a standard curve obtained by serial dilutions of a standard serum pool from 7- to 9-month-old (NZB × NZW)F_1 mice, containing 1,000 units/ml (5). DNA was obtained from calf thymus (Sigma). Chromatin was prepared as described in ref. 26. Briefly, nucleosomes were isolated by solubilizing chromatin from purified chicken erythrocyte nuclei with micrococcal nuclease. The solubilized chromatin was fractionated into sucrose gradients that were analyzed for monomers by using electrophoresis, and the appropriate fractions were dialyzed and pooled.

Analysis of T Cell Activation and T Cell Receptor (TCR) V_β Repertoires. To examine the activation states of $CD4^+$ T cells, aliquots of 10^6 spleen cells were double-stained with FITC-conjugated anti-CD4 mAb and phycoerythrin-conjugated anti-CD69 mAb. To analyze TCR V_β repertoires, spleen cells were stained with biotin-labeled mAbs to each TCR V_β repertoire (Pharmingen), followed by incubation with avidin-phycoerythrin and FITC-conjugated anti-CD4 mAb. All incubations were run for 30 min at 4°C, and the frequency of $CD4^+$ T cells with each TCR V_β repertoire per total $CD4^+$ T cells was calculated by using FACSTAR and CELLQUEST software.

Preparation of Retroviral Construct with Chromatin-Specific TCR Genes and Transduction to Splenocytes. Chromatin-specific TCR V_α and V_β DNA fragments were synthesized, using PCR based on the published sequences of the nucleosome-specific T cell line derived from the lupus-prone (SWR × NZB)F_1 mouse (27, 28), as described in ref. 29. These fragments were cloned into a pMXW retroviral vector (30) and transfected into PLAT-E packaging cell lines (31) by using FuGENE6 transfection reagent (Roche Diagnostics). The viral supernatant of transfected cells were placed on fibronectin-coated 24-well plates, and total spleen cells from 2-month-old (NZB × NZW)F_1 mice prestimulated for 48 h with Con A (10 μg/ml) and interleukin 2 (50 ng/ml) were added to the wells (1×10^6 cells per well). Cells were cultured further for 36 h to allow infection to occur.

Purification and Functional Analysis of Dendritic Cells (DCs). Spleen cells were treated with collagenase type IV (Sigma) and DNase I, and $CD11c^+$ cells were positively collected by passing spleen cells twice through MACS CD11c microbeads and magnetic separation columns. The purity (85% in average) of DCs was determined by flow cytometry with anti-CD11c-biotin, followed by streptavidin-phycoerythrin.

To analyze the potential of chromatin presentation, $CD4^+$ T cells were purified by negative selection, using MACS microbeads with anti-CD19, -CD11c, and -CD8 mAbs 24 h postinfection, and 2×10^4 cells per well of T cells were cocultured with 1×10^5 cells per well of irradiated $CD11c^+$ DCs in 96-well flat-bottom plates with 1 μg/ml chromatin. After 24 h of culture, the cells were pulse-labeled with 1 μCi (1 Ci = 37 GBq) of [^{3}H]thymidine per well (NEN) for 15 h, and the [^{3}H]thymidine incorporation was determined.

Statistical Analysis. Statistical analysis was performed by using Student's t test and the χ^2 test. $P < 5\%$ was considered to have a statistical significance.

Results

Establishment of Intra-MHC Recombinant-Congenic New Zealand Mice. By selective backcrossing, we first introduced the H-2^{g2} haplotype derived from the B10.GD strain into NZB (H-2^d) and NZW (H-2^z) and established H-2-congenic NZB.GD (20) and NZW.GD strains. H-2^{g2} has an intragenic recombination between d and b haplotype in the E gene and the H-2 haplotype is $K^dAb^dAa^dEb^dEa^bTnfa^bD^b$ (Table 1) (32). Because the Ea^b gene is defective, H-2^{g2} mice do not express E molecules (20). To establish the strain that carries the H-2 haplotype of $K^dAb^dAa^dEb^dEa^dTnfa^bD^b$, we conducted a search for the mouse with a spontaneously occurring intragenic recombination between Ea and $Tnfa$ in the progeny of NZB and NZB.GD crosses. In ≈3,000 meiosis, there was a single mouse carrying this recombination, and the recombination-congenic NZB line, provisionally designated NZB.GDr (H-2^{g2r}), was generated. This haplotype is valid to evaluate the effect of E molecule expression on the same $Tnfa^bD^b$ background. Table 1 summarizes the haplotypes of the intra-MHC-congenic New Zealand mouse and the related strains.

E Molecule Expression Levels in (NZB × NZW)F_1 Mice with Different Intra-H-2 Haplotypes. Congenic and recombinant-congenic New Zealand mice were crossed to obtain (NZB × NZW)F_1 mice with four different combinations of the H-2 haplotype (Table 1). Fig. 1 shows flow cytometric analyses for expression profiles of A, E, and D molecules on peripheral blood lymphocytes. As expected, although levels of A^d expression were almost identical, levels of E molecules differed significantly among these F_1 mice, i.e., full expression levels in H-$2^{d/d}$ homozygous, approximately one-half of expression levels in H-$2^{d/g2}$ and H-$2^{g2r/g2}$ heterozygous, and no expression in H-$2^{g2/g2}$ homozygous F_1 mice. Profiles of the class I D molecule expression showed that lymphocytes from H-$2^{d/g2}$ F_1 mice were positive for both D^d and D^b, whereas those from H-$2^{g2r/g2}$ and H-$2^{g2/g2}$ F_1 mice were positive for D^b and negative for D^d. As also shown in Fig. 1, E molecules in wild-type H-$2^{d/z}$ heterozygous F_1 mice were fully expressed. Because these F_1 mice are heterozygous H-$2^{d/z}$, the level of A^d and D^d expression was approximately one-half of that seen in the H-$2^{d/d}$ homozygote.

Comparisons of Disease Features. Fig. 2*A* compares cumulative incidences of proteinuria in wild-type H-$2^{d/z}$ heterozygous (NZB × NZW)F_1 mice with intact E molecule expression and four kinds of H-2-congenic (NZB × NZW)F_1 (H-$2^{d/d}$, H-$2^{d/g2}$, H-$2^{g2r/g2}$, and H-$2^{g2/g2}$) carrying identical homozygous $A^{d/d}$ molecules but different levels of E molecule expression. Compared with findings in wild-type F_1 mice, the incidence was markedly reduced in homozygous $A^{d/d}$ F_1 mice with intact E molecule expression (H-$2^{d/d}$). In a striking contrast, homozygous $A^{d/d}$ F_1 mice deficient in E expression (H-$2^{g2/g2}$) showed an early onset and a high incidence of proteinuria comparable to those found in the wild-type F_1 mice. Findings in H-$2^{d/g2}$ and H-$2^{g2r/g2}$ with one-half of E expression levels were in between. Together with the finding that heterozygous H-$2^{g2r/g2}$ and homozygous H-$2^{g2/g2}$ F_1 mice share the same H-2 haplotype except for the Ea subregion (Table 1), it is strongly suggested that the development of lupus nephritis in $A^{d/d}$ F_1 mice is down-regulated by E molecules in a dose-dependent manner.

As shown in Fig. 2*B*, the decrease in survival rate was associated with an increase in the incidence of proteinuria in all groups of mice. Whereas all H-$2^{g2/g2}$ F_1 mice and 90% of wild-type F_1 mice died of disease by 12 months of age, 80% of H-$2^{d/d}$ F_1 mice and ≈50% of H-$2^{d/g2}$ and H-$2^{g2r/g2}$ F_1 mice remained alive. In Fig. 2 *C* and *D*, we compare serum levels of IgG autoantibodies to DNA and to chromatin, respectively, in 6-month-old homozygous $A^{d/d}$ F_1 mice with different levels of E expression. Whereas H-$2^{g2/g2}$ F_1 mice lacking E molecules showed high levels of both autoantibodies, comparable to those found in wild-type F_1 mice, the levels were greatly reduced in mice expressing E molecules.

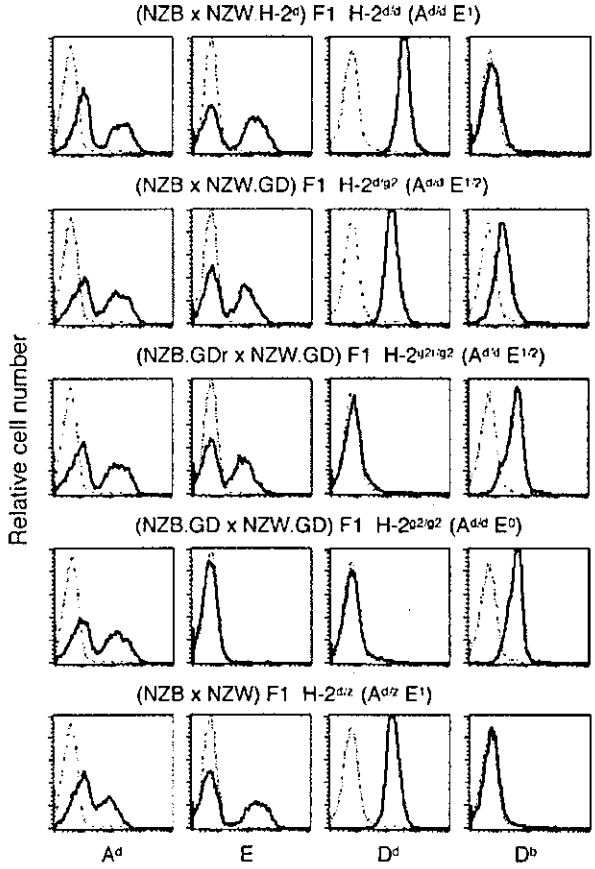

Fig. 1. Flow cytometry analysis for cell surface expression of A^d, E, D^d, and D^b molecules on peripheral lymphocytes in (NZB × NZW)F_1 mice with different H-2 haplotypes. The upper four groups of F_1 mice with homozygous $A^{d/d}$ showed the same expression level of A^d molecules, and the level in wild-type H-$2^{d/z}$ heterozygous F_1 mice was almost one-half of that seen in the former groups. When E molecule expression levels were examined with a mAb to a common determinant, H-$2^{d/g2}$ and H-$2^{g2r/g2}$ F_1 mice showed approximately one-half the level ($E^{1/2}$) of that seen in H-$2^{d/d}$ and wild-type H-$2^{d/z}$ F_1 mice (E^1). H-$2^{g2/g2}$ F_1 mice did not express E molecules (E^0). D^d expression levels in H-$2^{d/g2}$ and H-$2^{d/z}$ F_1 mice were approximately one-half of that seen in H-$2^{d/d}$ F_1 mice. D^b expression level in H-$2^{d/g2}$ F_1 mice was approximately one-half of that seen in H-$2^{g2r/g2}$ and H-$2^{g2/g2}$ F_1 mice.

Increase in Activated T Cells in E-Deficient Mice. Frequencies of $CD69^+$ activated $CD4^+$ T cells increase with age in (NZB × NZW)F_1 mice, as animals develop SLE (33). Fig. 3*A* compares frequencies of $CD69^+$ activated splenic $CD4^+$ T cells in total $CD4^+$ T cells among four groups of $A^{d/d}$ F_1 mice at 6 months of age. The frequency (mean ± SE) in E-negative H-$2^{g2/g2}$ F_1 mice (31.1 ± 8.6) was significantly higher than those found in three other groups of F_1 mice (11.0 ± 2.2 in H-$2^{d/d}$ F_1 mice, 14.2 ± 4.6 in H-$2^{d/g2}$ F_1 mice, and 17.2 ± 6.3 in H-$2^{g2r/g2}$ F_1 mice) ($P < 0.02$). Frequencies in H-$2^{d/g2}$ and H-$2^{g2r/g2}$ F_1 mice showed a tendency to be higher than those found in H-$2^{d/d}$ F_1 mice; however, there were no significant differences among the groups.

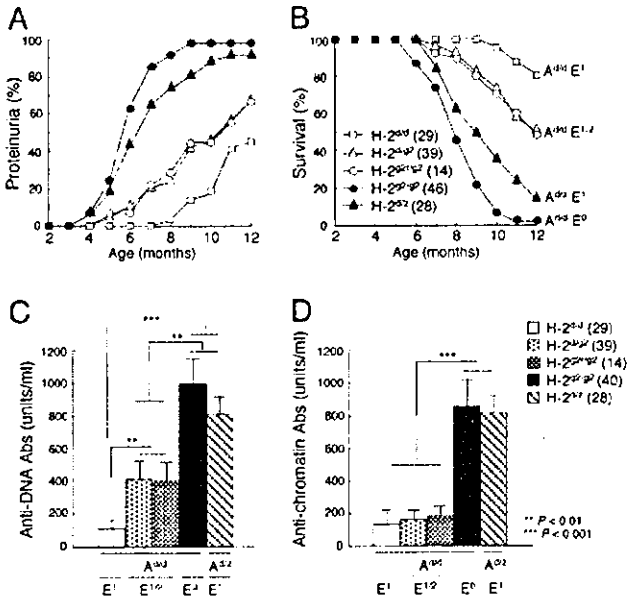

Fig. 2. Comparisons of the cumulative incidence of proteinuria (*A*), survival rate (*B*), and serum levels of IgG anti-DNA antibodies (*C*) and anti-chromatin antibodies (*D*) among F_1 mice with different H-2 haplotypes. The number of mice examined is shown in parentheses. H-$2^{g2/g2}$ F_1 showed a significantly higher incidence of proteinuria and a lower survival rate, as compared with three other $A^{d/d}$ F_1 strains ($P < 0.001$). Incidence of proteinuria and survival rate in H-$2^{d/d}$ F_1 mice were significantly reduced, as compared with H-$2^{d/g2}$ F_1 and H-$2^{g2r/g2}$ F_1 mice ($P < 0.01$). Compared with H-$2^{g2/g2}$ F_1 mice, wild-type H-$2^{d/z}$ F_1 mice showed a subtle but significantly lower incidence of proteinuria after 7 months of age ($P < 0.05$) and an improved survival rate after 9 months of age ($P < 0.05$). Serum levels of autoantibodies are compared at 6 months of age. Column and bar represent mean and SE, respectively. Asterisks indicate a significant difference.

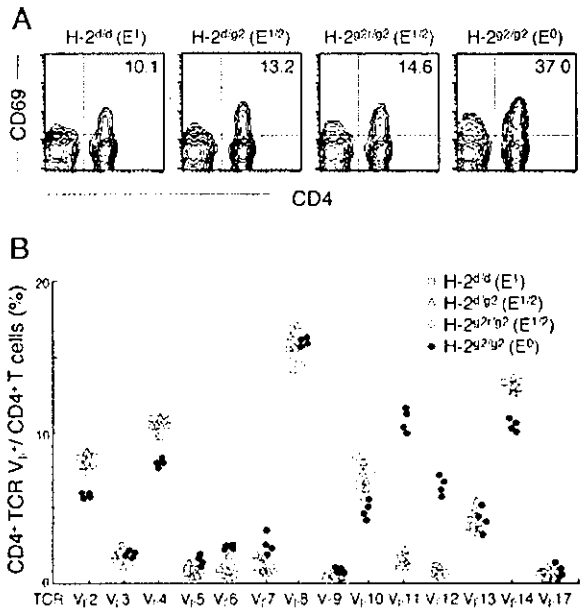

Fig. 3. Changes in splenic $CD4^+$ T cells among 6-month-old $A^{d/d}$ F_1 mice with different E molecule expression levels. (*A*) Representative flow cytometry profiles for the expression of activation marker CD69 on splenic $CD4^+$ T cells. Frequency of $CD69^+CD4^+$ T cells per total $CD4^+$ T cells is shown. (*B*) Comparisons of each TCR V_β repertoire frequency in splenic $CD4^+$ T cells. $V_\beta11$ and $V_\beta12$ repertoires were significantly higher in H-$2^{g2/g2}$ F_1 mice than those in other three F_1 mice ($P < 0.001$).

TCR V_β Repertoire Skewing in E-Deficient Mice. E molecule expression levels on thymic epithelial cells affect TCR V_β repertoire selection in the thymus (34–36). As shown in Fig. 3*B*, $V_\beta11$ and $V_\beta12$ repertoires in splenic $CD4^+$ T cells were negatively selected in E molecule-positive H-$2^{d/d}$, H-$2^{d/g2}$, and H-$2^{g2r/g2}$ F_1 mice, and there was no significant difference in these repertoire frequencies among the three groups. In contrast, significant proportions of $V_\beta11$ (mean and SE, 10.8 ± 0.2%) and $V_\beta12$ (6.0 ± 0.3%) repertoires were observed in E-negative H-$2^{g2/g2}$ F_1 mice.

Effects of E Molecule Expression on DC Function. Differences in haplotypes of class II molecules may affect autoimmune manifestations through the self-antigen presenting capacity of antigen-presenting cells. To determine whether the presence or absence of E molecules affects the potential for self-antigen presentation, we took advantage of a T cell proliferation assay against self-antigen. Splenic T cells from (NZB × NZW)F_1 mice were transfected *in vitro* with chromatin-specific TCR V_α and V_β, originally derived from a (SWR × NZB)F_1 mouse, which can recognize the immunodominant nucleosomal epitope (amino acids 71–94 in histone H4) in the context of $A^{d/d}$ (27, 28) and other A haplotype molecules (37). These T cells can reconstitute the specificity to the nucleosome (38). Such T cells and the T cells transfected with vector alone (mock) were cocultured with CD11c-positive splenic DCs obtained from (NZB × NZW)F_1 with different levels of E expression, in the presence of chromatin. As shown in Fig. 4, although DCs from $A^{d/d}$ F_1 mice with H-$2^{d/d}$, H-$2^{d/g2}$, and H-$2^{g2/g2}$ haplotypes induced significant levels of chromatin-specific T cell responses, there were no significant differences among the three groups of F_1 mice. Compared with findings in these $A^{d/d}$ F_1 mice, DCs from wild-type $A^{d/z}$ heterozygous (NZB × NZW)F_1 mice induced a significantly greater response of chromatin-specific T cells. Thus, it is suggested that, as compared with $A\alpha^d\beta^d$, $A^{d/z}$-unique $A\alpha^d\beta^z$ and/or $A\alpha^z\beta^d$ have an increased capacity of DCs to present chromatin and that the presence or absence of E molecules does not influence the potential of DCs for chromatin presentation.

Discussion

Our newly generated intra-MHC recombinant-congenic (NZB × NZW)F_1 mice make it feasible to examine the role of class II A and E molecules in the regulation of autoimmune disease, with disregard to the effect of other MHC genes such as *Tnfa* and class I D, which also have been implicated in autoimmune susceptibility (39, 40). The results clearly indicated that class II A and E serve as promoting and protective genetic elements, respectively.

H-$2^{d/z}$ heterozygosity has a strong impact on SLE in (NZB × NZW)F_1 mice, because the disease is largely reduced in H-$2^{d/d}$ and H-$2^{z/z}$ homozygous mice (2, 3, 5). This observation means that a combination of H-2-linked genes from both parents play a role in an epistatic manner. In this context, we earlier speculated that the polymorphic class II α and β chain genes from both parents may form F_1-unique mixed haplotype α/β heterodimers, such as $A\alpha^d\beta^z$ and $A\alpha^z\beta^d$, either of which may serve as a restriction element for self-reactive T cells (5). Consistent was the finding in the present studies that, compared with DCs from $A^{d/d}$ homozygous F_1 mice, DCs from wild-type $A^{d/z}$ (NZB × NZW)F_1 mice showed a greater likelihood of chromatin presentation to T cells. Because the antigen-presenting capacity was not influenced by the presence or absence of E molecules, class II A molecules can be attributed to this event. The importance of mixed haplotype α/β heterodimers also was supported by findings of Gotoh *et al.* (7), in

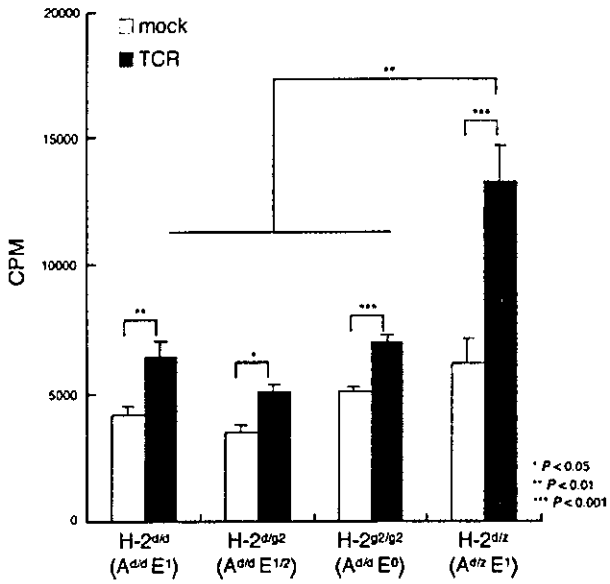

Fig. 4. The potential for chromatin presentation by CD11c-positive splenic cells from (NZB × NZW)F_1 mice with different H-2 haplotypes. Splenic T cells from (NZB × NZW)F_1 mice transfected with chromatin-specific TCR V_α and V_β or with vector alone (mock) were cocultured with CD11c-positive splenic DCs obtained from F_1 mice with different H-2 haplotypes, in the presence of chromatin, and T cell proliferative responses were compared. DCs from all these F_1 mice induced significant levels of chromatin-specific T cell responses; however, the potential of DCs for chromatin presentation was significantly higher in wild-type H-$2^{d/z}$ F_1 mice than that in other F_1 groups. Means and SE of three experiments are shown.

which the $A\alpha^d\beta^z$-restricted self-reactive T cell clone isolated from (NZB × NZW)F_1 mice had a potential to induce IgG anti-DNA antibodies *in vivo* (8). These F_1-unique mixed haplotype class II α/β heterodimers also may be involved in the aberrant selection of self-reactive T cells in the thymus. Based on studies by Braunstein and Germain (41), the assembly of $A\alpha$ and $A\beta$ chains of different haplotypes is under serious pairing restrictions. Thus, low expression levels of these heterodimers in the thymic epithelial cells may allow α/β heterodimer-restricted self-reactive T cells to escape from negative selection in the thymus.

In contrast to A molecules, the mixed-haplotype E molecules are not formed in most of the H-2 heterozygotes, because $E\alpha$ chains are usually nonpolymorphic (42). However, $E\alpha^z$ is unique among the $E\alpha$ chains of other haplotypes and has two amino acid substitutions in the α1 domain (43, 44). Thus, F_1 unique E molecules can be formed in H-$2^{d/z}$ F_1 mice. In this context, Nygard *et al.* (45) proposed the possible preferential formation of $E\alpha^d\beta^z$ mixed haplotype molecules and their involvement in the promotion of F_1 disease. However, evidence indicated that $E\alpha^d\beta^z$ molecules are protective rather than promoting (20).

The protective mechanism by E molecules remains elusive; however, several possibilities are suggested. First is the E-mediated clonal deletion model of self-reactive T cells in the thymus. It has been shown that T cells bearing TCR $V_\beta5$, $V_\beta11$, $V_\beta12$, and $V_\beta17a$ are eliminated in E-positive strains of mice (34–36), although the extent of negative selection is influenced by background genes (46–48). In this context, there are reports indicating that no clear-cut difference in the expression of TCR V_β repertoire was observed between E^+ and E^- transgenic NOD (16) as well as collagen-induced arthritis-susceptible B10.RQB3 mice (49), although the E transgene protected against the disease. Hence, the clonal deletion hypothesis for E-mediated protection of autoimmune disease has been dismissed in cases of these models. In the (NZB × NZW)F_1 genetic background, however, CD4 T cell repertoires bearing TCR $V_\beta11$ and $V_\beta12$ were significantly negatively selected in mice expressing E molecules. Thus, clonal deletion remains one possible mechanism at work in our mouse models.

Second is the determinant capture model. In *Ea^d*-transgenic BXSB mice, transgene-derived $E\alpha^d$ peptides bind to A^b molecules, possibly decreasing the use of A molecules for presentation of pathogenic self-peptides (18). Rudensky *et al.* (50) showed evidence for the binding of $E\alpha^d$ peptides to A^b molecules in a sequence analysis of peptides derived from the cell surface. This mechanism may be involved in the E-transgene-mediated protection of the collagen-induced arthritis model of $E\beta$-deficient B10.RQB3 mice (51, 52). However, such a mechanism may not be operative in our model, because the potential for chromatin presentation by $CD11C^+$ DCs was not affected by E molecules expressed in $A^{d/d}$ F_1 mice. This notion is in agreement with the finding by Nakano *et al.* (53) that antigen-presenting cells from both E^+ and E^- NOD mice can similarly stimulate diabetogenic T cells.

Third is the cytokine balance model. Hanson *et al.* (19) proposed that E molecule-mediated Th1/Th2 cytokine imbalance is one possible mechanism for the disease protection in $E\alpha^d$-transgenic NOD mice. Indeed, there is evidence that the differential MHC class II expression on antigen-presenting cells mediated by class II promoter polymorphism exerts a codominant effect on the Th1/Th2 cytokine balance (54, 55). In our preliminary studies, however, there was no clear difference in the potential of anti-CD3-stimulated T cells to produce IL-4 and IFN-γ between E^+ and E^- $A^{d/d}$ F_1 mice (data not shown).

An alternative is the signal transducer competition model, in which B cells may be the major cellular sites of E molecule-mediated autoimmune protection. Lang *et al.* (56) reported that antigen stimulation by means of the B cell antigen receptor on resting B cells induces association of MHC class II molecules with B cell antigen receptor-derived Ig-α/Ig-β heterodimers, which function as signal transducers on class II aggregation by the TCR. Because both A and E molecules physiologically associate with Ig-α/β heterodimers (56), when self-reactive B cells were stimulated by A-restricted T helper cells plus self-peptides, E molecules possibly associate competitively with Ig-α/β heterodimers. Hence, activation signals should be lower in E^+ than in E^- B cells. This idea well explains the observed dose dependency of E-mediated protection of SLE seen in the present studies.

Wild-type H-$2^{d/z}$ F_1 mice develop severe SLE, although they do express intact E molecules. This finding is in striking contrast to findings in H-$2^{d/d}$ F_1 mice that develop the disease only when lacking E molecules. Two mechanisms are thought to be involved. First, compared with H-$2^{d/d}$ F_1, the self-antigen-presenting capacity of DCs in H-$2^{d/z}$ F_1 is much higher, so that effects of E molecules may be insufficient for suppression. Alternatively, although not mutually exclusive, generation of H-$2^{d/z}$ F_1-unique self-reactive T cells restricted to haplotype-mismatched $A\alpha/\beta$ heterodimers in the thymus, as discussed above, may play a role in an E molecule-independent manner.

Taken collectively, our mouse models may provide means for further clarification of molecular mechanisms involved in the positive and negative regulation of autoimmune disease mediated by class II A and E molecules. Studies on the suppressive effect of E molecules are of particular importance, because one can apply this knowledge to future prophylactic and therapeutic approaches to autoimmune diseases.

We thank Prof. S. Matsushita (Saitama Medical School, Saitama, Japan) for helpful discussion and M. Ohara (Fukuoka, Japan) for language assistance. This work was supported in part by a Grant-in-Aid for

Scientific Research (B) for Scientific Research on Priority Areas and for Center of Excellence Research from the Ministry of Education, Science, Technology, Sports, and Culture of Japan and a grant from the Organization for Pharmaceutical Safety and Research (Japan).

1. Tsao, B. P. (2002) in *Dubois' Lupus Erythematosus*, eds. Wallace, D. J. & Hahn. B. H. (Lippincott Williams & Wilkins, Philadelphia), pp. 97–119.
2. Hirose, S., Nagasawa, R., Sekikawa, I., Hamaoki, M., Ishida, Y., Sato, H. & Shirai, T. (1983) *J. Exp. Med.* **158,** 228–233.
3. Hirose, S., Ueda, G., Noguchi, K., Okada, T., Sekigawa, I., Sato, H. & Shirai, T. (1986) *Eur. J. Immunol.* **16,** 1631–1633.
4. Kotzin, B. L. & Palmer, E. (1987) *J. Exp. Med.* **165,** 1237–1251.
5. Hirose, S., Kinoshita, K., Nozawa, S., Nishimura, H. & Shirai, T. (1990) *Int. Immunol.* **2,** 1091–1095.
6. Kono, D. H., Burlingame, R. W., Owens, D. G., Kuramochi, A., Balderas, R. S., Balomenos, D. & Theofilopoulos, A. N. (1994) *Proc. Natl. Acad. Sci. USA* **91,** 10168–10172.
7. Gotoh, Y., Takashima, T., Noguchi, K., Nishimura, H., Tokushima, M., Shirai, T. & Kimoto, M. (1993) *J. Immunol.* **150,** 4777–4787.
8. Tokushima, M., Koarada, S., Hirose, S., Gotoh, Y., Nishimura, H., Shirai, T., Miyake, K. & Kimoto, M. (1994) *Immunology* **83,** 221–226.
9. Murphy, E. D. & Roths, J. B. (1979) *Arthritis Rheum.* **22,** 1188–1194.
10. Merino, R., Fossati, L., Lacour, M., Lemoine, R., Higaki, M. & Izui, S. (1992) *Eur. J. Immunol.* **22,** 295–299.
11. Merino, R., Iwamoto, M., Fossati, L., Muniesa, P., Araki, K., Takahashi, S., Huarte, J., Yamamura, K. I., Vassalli, J. D. & Izui, S. (1993) *J. Exp. Med.* **178,** 1189–1197.
12. Hattori, M., Buse, J., Jackson, R., Glimcher, L., Dorf, M., Minami, M., Makino, S., Moriwaki, K., Kuzuya, H., Imura, H., *et al.* (1986) *Science* **231,** 733–735.
13. Acha-Orbea, H. & McDevitt, H. (1987) *Proc. Natl. Acad. Sci. USA* **84,** 2435–2439.
14. Nishimoto, H., Kikutani, H., Yamamura, K. & Kishimoto, T. (1989) *Nature* **328,** 432–434.
15. Lund, T., O'Reilly, L., Hutchings, P., Kanagawa, O., Simpson, E., Gravely, R., Chandler, P., Dyson, J., Picard, J., Edwards, A., *et al.* (1990) *Nature* **345,** 727–729.
16. Bohme, J., Schuhbaur, B., Kanagawa, O., Benoist, C. & Mathis, D. (1990) *Science* **249,** 293–295.
17. Labrecque, N., Madsen, L., Fugger, L., Benoist, C. & Mathis, D. (1999) *Immunity* **11,** 515–516.
18. Iwamoto, M., Ibnou-Zekri, N., Araki, K. & Izui, S. (1996) *Eur. J. Immmunol.* **26,** 307–314.
19. Hanson, M. S., Cetkovic-Cvrlje, M., Ramiya, V. K., Atkinson, M. A., Maclaren, N. K., Singh, B., Elliott, J. F., Serreze, D. V. & Leiter, E. H. (1996) *J. Immunol.* **157,** 1279–1287.
20. Hirose, S., Zhang, D., Nozawa, S., Nishimura, H. & Shirai, T. (1994) *Immunogenetics* **40,** 150–153.
21. Figueroa, F., Tewarson, S., Neufeld, E. & Klein, J. (1982) *Immunogenetics* **15,** 431–436.
22. Jongeneel, C. V., Acha-Orbea, H. & Blankenstein, T. (1990) *J. Exp. Med.* **171,** 2141–2146.
23. Jacob, C. O., Hwang, F., Lewis, G. D. & Stall, A. M. (1991) *Cytokine* **3,** 551–561.
24. Fujimura, T., Hirose, S., Jiang, Y., Kodera, S., Ohmuro, H., Zhang, D., Hamano, Y., Ishida, H., Fukukawa, S. & Shirai, T. (1998) *Int. Immunol.* **10,** 1467–1472.
25. Knight, J. G. & Adams, D. D. (1978) *J. Exp. Med.* **147,** 1653–1660.
26. Bates, D. L., Butler, P. J., Pearson, E. C. & Thomas, J. O. (1981) *Eur. J. Biochem.* **119,** 469–476.
27. Mohan, C., Adams, S., Stanik, V. & Datta, S. K. (1993) *J. Exp. Med.* **177,** 1367–1381.
28. Kaliyaperumal, A., Mohan, C., Wu, W. & Datta, S. K. (1996) *J. Exp. Med.* **183,** 2459–2469.
29. Fujio, K., Misaki, Y., Setoguchi, K., Morita, S., Kawahata, K., Kato, I., Nosaka, T., Yamamoto, K. & Kitamura, T. (2000) *J. Immunol.* **165,** 528–532.
30. Zufferey, R., Donello, J. E., Trono, D. & Hope, T. J. (1999) *J. Virol.* **73,** 2886–2892.
31. Morita, S., Kojima, T. & Kitamura, T. (2000) *Gene Ther.* **7,** 1063–1066.
32. Lilly, F. & Klein, Y. (1973) *Transplantation* **16,** 530–532.
33. Ishikawa, S., Akakura, S., Abe, M., Terashima, K., Chijiiwa, K., Nishimura, H., Hirose, S. & Shirai, T. (1998) *J. Immunol.* **161,** 1267–1273.
34. Kappler, J. W., Roehm, N. & Marrack, P. (1987) *Cell* **49,** 273–280.
35. Bill, J., Appel, V. & Palmer, E. (1988) *Proc. Natl. Acad. Sci. USA* **85,** 9184–9188.
36. Bill, J., Kanagawa, O., Woodland, D. L. & Palmer, E. (1989) *J. Exp. Med.* **169,** 1405–1419.
37. Shi, Y., Kaliyaperumal, A., Lu, L., Southwood, S., Sette, A., Michaels, M. A. & Datta, S. K. (1998) *J. Exp. Med.* **187,** 367–378.
38. Fujio, K., Okamoto, A., Tahara, H., Abe, M., Jiang, Y., Kitamura, T., Hirose, S. & Yamamoto, K. (2004) *J. Immunol.* **173,** 2118–2125.
39. Jacob, C. O. & McDevitt, H. O. (1988) *Nature* **331,** 356–358.
40. La Cava, A., Balasa, B., Good, A., van Gunst, K., Jung, N. & Sarvetnick, N. (2001) *J. Immunol.* **167,** 1066–1071.
41. Braunstein, N. S. & Germain, R. N. (1987) *Pro. Natl. Acad. Sci. USA* **84,** 2921–2925.
42. Mathis, D. J., Benoist, C. O., Williams, V. E., II, Kanter, M. R. & McDevitt, H. O. (1983) *Cell* **32,** 745–754.
43. Sciffenbauer, J., McCarthy, D. M., Nygard, N. R., Woulfe, S. L., Didier, D. K. & Schwartz, B. D. (1989) *J. Exp. Med.* **170,** 971–984.
44. Ogawa, S., Nishimura, H., Awaji, M., Nozawa, S., Hirose, S. & Shirai, T. (1990) *Immunogenetics* **32,** 63–67.
45. Nygard, N. R., McCarthy, D. M., Schiffenbauer, J. & Schwartz, B. D. (1993) *Immunol. Today* **14,** 53–56.
46. Kappler, J. W., Staerz, U., White, J. & Marrack, P. (1987) *Nature* **332,** 35–40.
47. MacDonald, H. R., Schneider, R., Lees, R. K., Howe, R. C., Acha-Orbea, H., Festenstein, H., Zinkernargel, R. M. & Hengartner, H. (1988) *Nature* **332,** 40–45.
48. Pullen, A. M., Marrack, P. & Kappler, J. W. (1988) *Nature* **335,** 796–801.
49. Gonzalez-Gay, M. A., Nabozny, G. H., Bull, M. J., Zanelli, E., Douhan, J., III, Griffiths, M. M., Glimcher, L. H., Luthra, H. S. & David, C. S. (1994) *J. Exp. Med.* **180,** 1559–1564.
50. Rudensky, A. Y., Preston-Hurlburt, P., Hong, S. C., Barlow, A. & Janeway, C. A., Jr. (1991) *Nature* **353,** 622–627.
51. Gonzalez-Gay, M. A., Zanelli, E., Krco, C. J., Nabozny. G. H., Hanson, J., Griffiths, M. M., Luthra, H. S. & David, C. S. (1995) *Immunogenetics* **42,** 35–40.
52. Gonzalez-Gay, M. A., Zanelli, E., Khare, S. D., Krco, C. J., Griffiths, M. M., Luthra, H. S. & David, C. S. (1996) *Immunogenetics* **44,** 377–384.
53. Nakano, N., Kikutani, H., Nishimoto, H. & Kishimoto, H. (1991) *J. Exp. Med.* **173,** 1091–1097.
54. Guardiola, J., Maffei, A., Lauster, R., Mitchison, N. A., Accolla, R. S. & Sartoris, S. (1996) *Tissue Antigens* **48,** 615–625.
55. Baumgard, M., Moos, V., Schuhbauer, D. & Müller, B. (1998) *Proc. Natl. Acad. Sci. USA* **95,** 6936–6940.
56. Lang, P., Stolpa, J.C., Freiberg, B. A., Crawford, F., Kappler, J., Kupfer, A. & Cambier, J. C. (2001) *Science* **291,** 1537–1540.